

University of Windsor

Scholarship at UWindsor

Great Lakes Institute for Environmental
Research Publications

Great Lakes Institute for Environmental
Research

1-1-2019

Responses of phytoplankton assemblages to iron availability and mixing water masses during the spring bloom in the Oyashio region, NW Pacific

T. Isada
Hokkaido University


A. Hattori-Saito
Hokkaido University


H. Saito
Tohoku National Fisheries Research Institute, FRA

Y. Kondo
Graduate School of Agricultural and Life Sciences The University of Tokyo

J. Nishioka
Hokkaido University

Follow this and additional works at: <https://scholar.uwindsor.ca/glierpub>

 See next page for additional authors

 Part of the [Biochemistry, Biophysics, and Structural Biology Commons](#), [Biodiversity Commons](#), [Biology Commons](#), and the [Marine Biology Commons](#)

Recommended Citation


Isada, T.; Hattori-Saito, A.; Saito, H.; Kondo, Y.; Nishioka, J.; Kuma, K.; Hattori, H.; McKay, R. M.L.; and Suzuki, K.. (2019). Responses of phytoplankton assemblages to iron availability and mixing water masses during the spring bloom in the Oyashio region, NW Pacific. *Limnology and Oceanography*, 64 (1), 197-216. <https://scholar.uwindsor.ca/glierpub/554>

This Article is brought to you for free and open access by the Great Lakes Institute for Environmental Research at Scholarship at UWindsor. It has been accepted for inclusion in Great Lakes Institute for Environmental Research Publications by an authorized administrator of Scholarship at UWindsor. For more information, please contact scholarship@uwindsor.ca.

Authors

T. Isada, A. Hattori-Saito, H. Saito, Y. Kondo, J. Nishioka, K. Kuma, H. Hattori, R. M.L. McKay, and K. Suzuki

Responses of phytoplankton assemblages to iron availability and mixing water masses during the spring bloom in the Oyashio region, NW Pacific

T. Isada, ^{1*} A. Hattori-Saito,¹ H. Saito,^{2,3} Y. Kondo,^{4,5} J. Nishioka, ^{1,6} K. Kuma,⁷ H. Hattori,⁸
R. M. L. McKay,⁹ K. Suzuki^{1,10}

¹Graduate School of Environmental Science, Hokkaido University, Sapporo, Hokkaido, Japan

²Tohoku National Fisheries Research Institute, Shiogama, Japan

³Atmosphere and Ocean Research Institute, The University of Tokyo, Kashiwa, Japan

⁴Graduate School of Agricultural and Life Sciences, The University of Tokyo, Tokyo, Japan

⁵Faculty of Fisheries and Environmental Sciences, Nagasaki University, Nagasaki, Japan

⁶Institute of Low Temperature Science, Hokkaido University, Sapporo, Japan

⁷Faculty of Fisheries Sciences, Hokkaido University, Hakodate, Hokkaido, Japan

⁸Department of Marine Biology and Sciences, Hokkaido Tokai University, Sapporo, Japan

⁹Department of Biological Sciences, Bowling Green State University, Bowling Green, Ohio

¹⁰Faculty of Environmental Earth Science, Hokkaido University, Sapporo, Hokkaido, Japan

Abstract

Spring phytoplankton blooms play a major role in the carbon biogeochemical cycle of the Oyashio region, western subarctic Pacific, where the seasonal biological drawdown effect on seawater $p\text{CO}_2$ is one of the greatest among the world's oceans. However, the bloom often terminates before depleting macronutrients, and the initiation and magnitude of the bloom is heterogeneous. We conducted a high resolution taxonomic and physiological assessment of phytoplankton in relation to the different physicochemical water masses of Coastal Oyashio Water (COW), Oyashio water (OYW), and modified Kuroshio water (MKW) in the Oyashio region from April to June 2007. Massive diatom blooms were found in April. Then, chlorophyll *a* concentration, cell abundance of diatom taxa, and the maximum photosystem II photochemical efficiency (F_v/F_m) were positively correlated with the mixing ratios of COW, suggesting that the spring bloom in April was strongly affected by the intrusion of COW. In the OYW, intensive blooms occurred from the middle of May under low dissolved iron (DFe) concentration (< 0.26 nM). Redundancy analysis showed that while diatom blooms accompanied by COW were related to DFe concentration, this was not the case in the OYW. These results indicated that diatoms in the OYW possess different iron adaptation strategies compared with diatoms in the water masses affected by COW. This led to the spatial heterogeneity of the Oyashio spring bloom. The results presented here demonstrate that water mass characterization with detailed assessments of phytoplankton taxonomy and physiological status can improve our understanding of marine ecosystems.

In the subarctic Pacific, mesoscale in situ iron (Fe) enrichment experiments have revealed that iron availability influences phytoplankton productivity and species composition both in the western (Tsuda et al. 2003, 2007) and eastern (Boyd

et al. 2004) oceanic regions (Boyd et al. 2007). However, in terms of the seasonal changes in natural conditions, the western subarctic Pacific (WSP) shows high-amplitude seasonal cycles in nutrients and plankton biomass as compared with the eastern subarctic Pacific (the Alaskan Gyre) (Harrison et al. 1999, 2004; Saito et al. 2002). In the Oyashio region of the WSP, which is located off the coast of Hokkaido Island, Japan, massive diatom blooms occur every spring (Kasai et al. 1997; Chiba et al. 2004; Tsuda et al. 2005; Okamoto et al. 2010; Suzuki et al. 2011). The phytoplankton assemblages during the spring bloom in the Oyashio region possess higher light utilization efficiency of photosynthesis and primary productivity (Shiomoto 2000; Isada et al. 2009, 2010), which contributes to the highest biological utilization effect on seawater $p\text{CO}_2$ in the world ocean

*Correspondence: t-isada@fsc.hokudai.ac.jp

Present address: ³Akkeshi Marine Station, Field Science Center for Northern Biosphere, Hokkaido University, Akkeshi, Hokkaido, Japan

This is an open access article under the terms of the Creative Commons Attribution-NonCommercial-NoDerivs License, which permits use and distribution in any medium, provided the original work is properly cited, the use is non-commercial and no modifications or adaptations are made. Additional Supporting Information may be found in the online version of this article.

(Takahashi et al. 2002; Chierici et al. 2006) and high biological production (Taniguchi 1999; Sakurai 2007; Ikeda et al. 2008; FAO 2016). Nosaka et al. (2017) reported that diatoms during the spring bloom in the Oyashio region are the main producer of transparent exopolymer particles (TEPs) that affect the efficiency of the biological carbon pump. Therefore, understanding the spatiotemporal changes in spring bloom dynamics is essential for better characterizing the biogeochemical and ecosystem processes in the Oyashio region.

The high biological production in the Oyashio region is considered to be supported by elevated iron supply from intermediate water derived from the Sea of Okhotsk along with atmospheric dust deposition which makes the Oyashio region different from other high-nutrient, low-chlorophyll (HNLC) regions in the subarctic Pacific (Nishioka et al. 2007, 2011). Suzuki et al. (2002) and Nishioka and Obata (2017) have reported the high-west to low-east gradients in iron concentration in the subarctic Pacific. Although the spring diatom bloom in the Oyashio region is a regular key event of the biological production, the bloom often terminates with incomplete depletion of macronutrients (Saito et al. 2002), suggesting that other factors, for example, iron availability and zooplankton grazing, can regulate spatiotemporal changes in the spring bloom. Iron is now recognized as a limiting factor for phytoplankton growth in not only HNLC regions but also some coastal regions (e.g., Hutchins and Bruland 1998; Suzuki et al. 2014) where diatom blooms sometimes occurs (Moore et al. 2006). Diatoms have well evolved iron-related metabolisms (Groussman et al. 2015; Marchetti and Maldonado 2016), for example, Fe (and Cu) metalloprotein substitution of ferredoxin (Fd)/flavodoxin (Fld) and cytochrome c_6 /plastocyanin, and an Fe storage capacity (ferritin). Based on immunological Fd (iron-containing protein)/Fld (iron-free protein) assays, Hattori-Saito et al. (2010) showed that microplankton-sized (hereafter micro-sized) diatoms during the spring in the Oyashio region were stressed by iron deficiency. However, their snapshot observation was insufficient to evaluate the iron stress of diatoms through the whole span of the spring bloom (Hattori-Saito et al. 2010).

The hydrographic structure during spring in the Oyashio region often becomes complex, influenced by varying mixtures of the Oyashio water (OYW), Coastal Oyashio water (COW), and modified Kuroshio Water (MKW) with different physicochemical properties (Kono and Sato 2010). The Oyashio is a cold western boundary current in WSP, stemming from both the East Kamchatka Current and the Okhotsk Sea Mode Water (Yasuda 2003, 2004). The OYW reaches to the northeast coast of Japan, and then mixes with warm saline water transported by the Kuroshio, an alternative Pacific western boundary current. In the area of converging waters from the Oyashio and Kuroshio, several meso-scale eddies, such as Kuroshio warm-core rings, distribute (Yasuda 2003; Itoh and Yasuda 2010). The warm core rings separated from the Kuroshio carry the MKW with lifespans of more than 1 yr into the Oyashio region. The COW, a water mass which is colder and less saline than OYW, is distributed along the

southeast coast of Hokkaido, Japan from January to May (Kono and Sato 2010; Sakamoto et al. 2010; Kusaka et al. 2013). The COW is considered to be independent of the OYW and affected by coastal waters from the Sea of Okhotsk (Ohtani et al. 1971). Accordingly, the COW forms a density front to the OYW this is 10 km wide near the shelf break from winter to spring (Sakamoto et al. 2010). Thus, the confluence of two or three dominant water masses in the Oyashio region produces the complex oceanographic conditions (Yasuda 2003, 2004; Itoh and Yasuda 2010; Kono and Sato 2010). Furthermore, chlorophyll (Chl) *a* concentration derived from ocean color remote sensing clearly demonstrates the spatiotemporal heterogeneity of spring phytoplankton bloom in the Oyashio region (Okamoto et al. 2010). However, little is known about the factors regulating phytoplankton physiology and spatial heterogeneity of phytoplankton biomass during the spring bloom in the Oyashio region owing to a lack of extensive in situ observation (Yoshie et al. 2010; Shiozaki et al. 2014). Because the spring bloom is an important event for the biological carbon pump and supports the energy transfer to a wide variety of commercially valuable fishes in the Oyashio region, clarifying the factors controlling bloom heterogeneity in relation to the mixing water masses would accelerate further understanding of the Oyashio ecosystem.

The objectives of this study were (1) to examine iron stress of micro-sized diatoms and (2) to clarify the factor(s) regulating the spatiotemporal heterogeneity in phytoplankton assemblages and photophysiology in relation to the complex water masses during the spring bloom in the Oyashio region. To this end, we conducted high-frequency Eulerian observations at a fixed station in April 2007 followed by spatiotemporal monitoring of six sampling stations from May to June 2007 in the Oyashio region.

Material and methods

Field campaigns

Two field campaigns (Oceanic Ecosystems Comparison Subarctic-Pacific-West: OECOS [Ikeda et al. 2010] and Blooming Plankton Succession Study in the Oyashio Marine Ecosystem: BLOSSOM) were carried out in the Oyashio region of the northwest Pacific Ocean. Regarding the OECOS cruise, the Eulerian observations were conducted at the station (Stn.) A5 (Fig. 1) of the monitoring “A-Line” from 05 April 2007 to 01 May 2007 aboard the R/V *Hakuho Maru* (JAMSTEC, Japan). In the BLOSSOM cruises, spatiotemporal monitoring was conducted at six stations (Fig. 1: Stns. A4, A7, B1, B2, B3, and B4) along the monitoring “A-Line” and “B-Line” during 09–21 May 2007 and 04–14 June 2007 aboard the FR/V *Wakataka Maru* (Fisheries Research Agency, Japan).

Seawater sampling

OECOS

Seawater was sampled using acid-cleaned Teflon-coated Niskin-X bottles mounted on a conductivity–temperature–

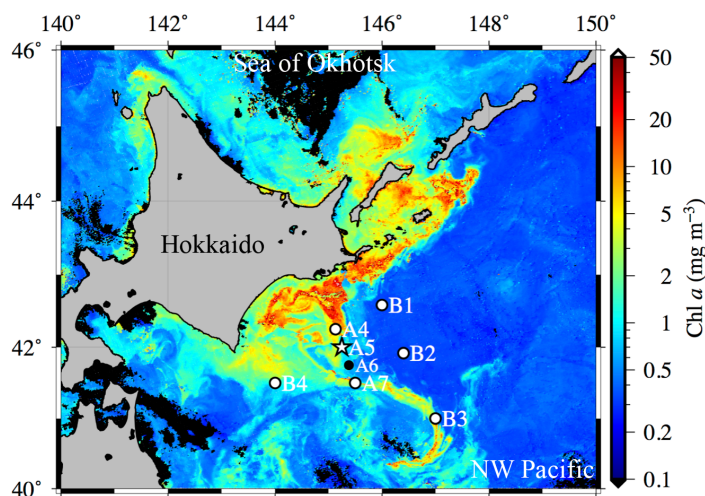


Fig. 1. Sampling stations in the Oyashio region of the NW Pacific, superimposed on composite image (from 05 April 2007 to 11 April 2007) of Chl *a* concentration derived from MODIS/aqua with 1 km resolution (<https://oceancolor.gsfc.nasa.gov>). Star and closed white circles represent the stations during the OECOS cruise in April 2007 and the BLOSSOM cruises in May and June 2007, respectively. Black symbol represents the sampling station (Stn. A6) conducted only 12 April 2007 when samples for HPLC, *PE* curve experiment, and F_v/F_m measurements of overall phytoplankton assemblage were taken.

depth carousel multi-sampler (CTD-CMS) system connected via a titanium armored cable. First, waters samples for macronutrients and Chl *a* concentration were obtained from nine depths ranging from 5 m to 100 m. Samples for dissolved iron (leachable iron in 0.22 μm filtrate; hereafter DFe) concentration and cell densities of diatoms were also collected from 5 m depth. Simultaneously, samples for protein assay of ferredoxin (Fd) and flavodoxin (Fld) in the micro-sized (20–200 μm) diatoms and the maximum photosystem II (PSII) photochemical quantum efficiency (F_v/F_m) of the total micro-sized (20–200 μm) phytoplankton including diatoms described below were obtained from the seawater intake (ca. 5 m) of the research vessels. After sampling at fixed depths, MER2040/2041 spectroradiometers (Biospherical Instruments) were deployed to measure vertical profiles of photosynthetic available radiation (PAR) and determine five optical depths (OD) (60%, 30%, 10%, 5%, and 1% ODs of incident PAR at the surface). Next, samples for nutrient concentration, Chl *a* concentration, and phytoplankton pigments were taken from the surface (ca. 2–5 m depth) and 5 ODs. Samples for photosynthesis versus irradiance (*PE*) curve experiments and F_v/F_m measurements of the overall phytoplankton assemblage were collected from the surface and 5% OD. Sampling at fixed- and optical depths during the OECOS cruise was conducted at ~ 9:00 and noon (local time), respectively. On 12 April, water samples for phytoplankton pigments, *PE* curve experiments, and F_v/F_m measurements of overall phytoplankton assemblage were taken only at the surface at Stn. A6 (Fig. 1). DFe data during the OECOS cruise were obtained from Nakayama et al. (2010). Daily PAR data above the sea surface

were obtained from Isada et al. (2010). Macronutrient (nitrate plus nitrite, phosphate, and silicate) concentrations were measured with a continuous flow analyzer (QuAatro, Bran + Luebbe).

BLOSSOM

After measuring the vertical profiles of PAR with profiling radiometers (PRR600/610, Biospherical Instruments), samples were obtained from 5 m depth and 4–5 ODs between early morning and noon using acid-cleaned Niskin bottles attached to a CTD-CMS. Then, samples for Fd/Fld protein of the micro-sized diatoms and F_v/F_m of the total micro-sized phytoplankton were obtained from the seawater intake (ca. 5 m) of the research vessels in the same manner as during OECOS as described above. Samples for DFe analysis were collected from ca. 10 m using an acid-cleaned Teflon-coated 10 L Niskin-X bottle attached to Kevlar line. The DFe samples were measured following the methods described in Obata et al. (1993) and Nishioka et al. (2007, 2011). Daily PAR data above the sea surface were taken from Isada et al. (2010). Macronutrient concentrations were measured with a continuous flow analyzer (TRAACS 800, Bran + Luebbe).

Chl *a* concentration

Samples (150–200 mL) were filtered through glass-fiber filters (Whatman GF/F, 25 mm diameter) under gentle vacuum (< 0.013 MPa). Chl *a* pigment was extracted by 6 mL of *N,N*-dimethylformamide (DMF) in a glass tube at -20°C for more than 24 h (Suzuki and Ishimaru 1990) on board. For the filters during the BLOSSOM cruises, the filters were stored at -80°C in a deep freezer or in liquid nitrogen until analysis on land. The Chl *a* concentration was measured with a Turner Designs fluorometer (model 10-AU) based on the non-acidification method (Welschmeyer 1994).

Phytoplankton pigments and CHEMTAX analysis

Samples (250–1000 mL) were filtered onto glass-fiber filters (Whatman GF/F, 25 mm diameter) under gentle vacuum (< 0.013 MPa). The filters were stored in the same way as described above for the Chl *a* analysis during the BLOSSOM cruises. The frozen filters were cut into small pieces, soaked in 3 mL of DMF in an amber glass vial, and sonicated with an ultrasonic homogenizer (SONIFIER model 250, Branson) for 30 s on ice. Phytoplankton pigments were quantified with high-performance liquid chromatography (HPLC) following Wright et al. (1991). Further details of the analytical procedure are described by Suzuki et al. (2005).

To estimate phytoplankton community composition based on HPLC pigments, chemotaxonomic analysis of phytoplankton pigments was applied using the program CHEMTAX (v1.95) with multiple starting points (Wright et al. 2009). The seed ratio matrix provided by Suzuki et al. (2011) (Supporting Information) was used for CHEMTAX analysis. Pigment data were separated for three layers (surface–60% OD [$n = 32$],

30–10% OD [$n = 44$], and 5–1% OD [$n = 50$]) and were analyzed respectively. A series of 60 pigment ratio matrices created by randomly multiplying each ratio of the seed ratio matrix was used to calculate the optimized initial matrices. The average values of the six best output solutions were used to determine the initial ratio matrix. Subsequently, the final ratios matrix was calculated by CHEMTAX.

Identification and enumeration of diatoms

The seawater (500 mL) was stored in 0.2% (final concentration) neutralized paraformaldehyde at 4°C until enumeration with scanning electron microscope (SEM, JMS-840A, JOEL) in the laboratory on land. Preparation and analysis of samples for SEM were carried out according to Hattori et al. (2004) and Nosaka et al. (2017). An aliquot (5–20 mL) of the sample was filtered through 1 μm pore size Nuclepore membrane filter under a vacuum less than 0.026 MPa. The membrane filter was rinsed with distilled water to remove all salt and then dried for several hours in an oven between 40°C and 60°C. Identification and enumeration of diatoms were made by SEM with 1000X magnification. The half area of the membrane (> 20 mm²) was examined. However, when the number of cells counted in the area was < 1000, the whole area was examined. Diatoms species were identified following Tomas (1997).

Immunological assays for ferredoxin and flavodoxin

Samples were pre-filtered using 200 μm nylon mesh to remove larger plankton and subsequently concentrated using a 20 μm nylon mesh plankton net. Next, cells were filtered onto 5 μm nylon mesh under low vacuum (< 0.0065 MPa), rinsed from the nylon mesh with Whatman GF/F-filtered seawater, and centrifuged to concentrate into a pellet. Cell pellet were stored in a deep freezer (–80°C) or in liquid nitrogen until analysis on land. Fd and Fld proteins of micro-sized diatoms were analyzed following Suzuki et al. (2009, 2014) and Hattori-Saito et al. (2010). The intensity of flavodoxin in each band was normalized to that of the positive control for flavodoxin, which was derived from an Fe-deficient centric diatom *Thalassiosira nordenskiöldii* isolated from the NW subarctic Pacific (Suzuki et al. 2009).

Pulse amplitude modulation (PAM) fluorometry measurement

Seawater samples (ca. 50 mL) of the entire phytoplankton assemblages were dispensed into acid-cleaned amber polyethylene bottles to protect them from light and stored in the dark at the sea surface temperature for ca. 30 min. Regarding samples for the total micro-sized phytoplankton, the cell pellets collected in the same way as described above for immunological Fd/Fld assay were suspended with Whatman GF/F-filtered seawater and then transferred into acid-cleaned amber polyethylene bottles. The minimum (F_0) and maximum (F_m) fluorescence of the samples was measured with a pulse amplitude modulated fluorometer (Water-PAM, Heinz Walz GmbH). F_0

and F_m were measured by the measuring light (peaking at 650 nm) and saturation pulse with the light intensity of ca. 4000 $\mu\text{mol photons m}^{-2} \text{s}^{-1}$ for 0.8 ms (peaking at 660 nm) of the PAM with red LEDs to estimate F_v/F_m . The values of F_0 , F_m , and F_v/F_m were obtained with WinControl software. The measurements were conducted two to four times in each sample, and the obtained values were averaged according to the methods of Suzuki et al. (2014).

Photosynthesis versus irradiance (PE) curve experiment

Incubation for examining PE parameters of the entire phytoplankton assemblage was performed using the ¹³C labeling method (Hama et al. 1983). Seawater sampling, incubation, and measurement of the particulate organic carbon (POC) and the isotope ratio of ¹²C and ¹³C abundance of the sample using mass spectrometer coupled with elemental analyzer (EA-MS) were conducted following the procedures described by Isada et al. (2013). Seawater samples dispensed into 10 acid clean polystyrene bottles (275 mL) were exposed to light intensities ranging from 2 $\mu\text{mol photons m}^{-2} \text{s}^{-1}$ to 3400 $\mu\text{mol photons m}^{-2} \text{s}^{-1}$ for surface samples and from 1 $\mu\text{mol photons m}^{-2} \text{s}^{-1}$ to 380 $\mu\text{mol photons m}^{-2} \text{s}^{-1}$ for the 5% OD samples over a 2 h period at the sea surface temperature. Total dissolved inorganic carbon (DIC) used to calculate the photosynthetic rates was measured with a CO₂ coulometer (CM5012, UIC) (Isada et al. 2010). The photosynthetic rates were calculated according to the method of Hama et al. (1983) and were normalized to the Chl *a* concentration measured with HPLC. The calculated values were fitted by the negative exponential function with photoinhibition proposed by Platt et al. (1980). Curve fitting was conducted with the R software v. 3.5.0 (R Core Team 2018) using the phytotools (Silsbe and Kromkamp 2012; Silsbe and Malkin 2015) package to obtain the Chl *a* specific maximum photosynthetic rate ($P_{\text{max}}^{\text{B}}$, mg C mg Chl $\text{a}^{-1} \text{h}^{-1}$) and the initial slope of the curve (α^{B} , (mg C mg Chl $\text{a}^{-1} \text{h}^{-1}) (\mu\text{mol photons m}^{-2} \text{s}^{-1})^{-1}$). Additionally, the light saturation index (E_k , $\mu\text{mol photons m}^{-2} \text{s}^{-1}$) and the maximum quantum yield for carbon fixation (Φ_{cmax} , mol C mol photons⁻¹) were calculated (i.e., $E_k = P_{\text{max}}^{\text{B}} / \alpha^{\text{B}}$ and $\Phi_{\text{cmax}} = 0.0231\alpha^{\text{B}} / \bar{a}_{\text{ph}}^*$). For the Φ_{cmax} calculation, the spectrally weighted Chl *a* specific absorption coefficient of phytoplankton at the wavelengths from 400 to 700 nm, \bar{a}_{ph}^* (m² mg Chl a^{-1}), was calculated from the relative spectral irradiance of the incubator lamp and the Chl *a* specific phytoplankton absorption coefficient ($a_{\text{ph}}^*(\lambda)$), which was obtained from Isada et al. (2010).

Water mass classification

To clarify the temporal changes in contributions of the OYW, COW, and MKW to each water mass observed at Stn. A5 during the OECOS cruise, the mixing ratio proposed by Kono and Sato (2010) was calculated using the potential temperature and salinity of these water masses (OYW: 0.994°C, 33.168, COW: 1.21°C, 32.847, MKW: 8.655°C, 33.837) as end-members. However, the method cannot be applied to an

observed water mass when temperature and salinity of the observed water mass is not within the triangle created with the end-members in a temperature–salinity (T–S) scatter diagram (see Figs. 2–3) because of negative values of the ratio. Then, water masses were simply categorized into OYW (temperature < 7°C, salinity 33.0–33.7), COW (temperature < 2°C, salinity < 33.0), or MKW following Hanawa and Mitsudera (1987) and Kusaka et al. (2013).

Statistical analyses

Shannon Wiener diversity index (H') values were estimated for the diatom species identified by SEM. Additionally, a hierarchical cluster analysis was used to categorize the diatom species into specific groups. In this study, the cluster analysis based on the diatoms abundance was performed using Bray–Curtis dissimilarity and unweighted pair group method using arithmetic averages (UPGMA). Redundancy analysis (RDA) was also performed to examine the relationships between the cell concentrations of each diatom and the environmental variables at the surface. Cell concentrations of each diatom species were used as biotic variables. The environmental variables included temperature, salinity, nitrate, phosphate, silicate, DFe, and mixed layer depth (MLD) which was estimated using the threshold values of potential density ($\Delta\sigma_\theta = 0.125$) relative to those at 10 m depth (Levitus 1982; Suga et al. 2004). To eliminate the effect of extreme data on ordination scores, all of these data were $\log(x + 1)$ transformed before analysis. Kendall rank correlation coefficient was calculated to examine the relationships between biotic parameters (Chl a concentration, total diatom abundance, cell concentrations of each diatom species, photosynthetic parameters, and flavodoxin (Fld) and environmental variables including the mixing ratio. All statistical analyses were conducted with the R software v. 3.5.0 (R Core Team 2018) with psych (Revelle 2018) and vegan (Oksanen et al. 2018) packages.

Results

Hydrography

Hydrographic condition, satellite images of SST and Chl a concentration, and both macronutrient and iron concentrations during the OECOS cruise are detailed in Kono and Sato (2010), Nakayama et al. (2010), and Sugie et al. (2010) and therefore are only briefly mentioned here. The hydrography observed at the fixed station (Stn) A5 of the *A-Line* during OECOS was not a consistent water mass (Table 1; Fig. 2). In the beginning of OECOS cruise during 06 April 2007–12 April 2007, water masses at Stn. A5 were mainly occupied by COW. Then, higher Chl a concentrations with the maximum 39 mg m^{-3} and dissolved iron (DFe) concentrations were found within the mixed layer, and the euphotic depth (Z_{eu}) was shallow during 06 April–07 April (Table 1; Fig. 2b). After that, the MKW flowed into Stn. A5, and lower Chl a concentrations were found especially between 13 April and 19 April. Subsequently, the

COW with higher Chl a concentrations was dominant again between 20 April and 26 April. The MKW was encountered again from 30 April to 01 May at the end of OECOS cruise when Chl a levels were low, but macronutrients concentrations were relatively high. The average value of DFe concentration during OECOS was 0.31 ± 0.11 nM (Table 1). The average of daily photosynthetically available radiation (PAR) on deck during OECOS was 38.3 ± 9.9 mol photons $m^{-2} d^{-1}$. Throughout the OECOS cruise, Chl a levels were negatively correlated with temperature ($\tau = -0.76$, $p < 0.001$, $n = 17$), salinity ($\tau = -0.67$, $p < 0.01$, $n = 17$), and MLD ($\tau = -0.51$, $p < 0.05$, $n = 17$). As a result, Chl a concentrations were positively and negatively correlated with the contribution of COW and MKW to the observed water masses, respectively (Table 3).

During the BLOSSOM cruises in May and June 2007, temperature and salinity values of the observed water masses in the surface layer (from the surface to ca. 50 m) were located outside the triangle of three water masses in the T–S scatter diagram (Fig. 3), indicating that water masses during BLOSSOM were clearly distinct from those during OECOS and that the mixing ratio analysis was not applicable to BLOSSOM data. Therefore, water masses during BLOSSOM were classified following Hanawa and Mitsudera (1987) and Kusaka et al. (2013). As a result, all stations except at Stns. A4–6 in June and B4–4 in May were categorized into the OYW (Table 1). Water mass at Stns. A4–6 and B4–4 possessed higher temperature and salinity values, so that those were categorized as MKW. Of stations categorized into the OYW, water masses at Stns. B1 and B2 (Fig. 3b, c) in the eastern part of the Oyashio region were a consistent water mass of OYW with relatively high surface temperatures (Table 1). Chl a concentrations at these stations were relatively low in early May 2007 (i.e., Stns. B1–4 and B2–4, Table 1), although ample macronutrients were found. However, the Chl a concentrations dramatically increased at these stations (i.e., Stns. B1–5 and B2–5) after 5 d from the first observation, despite almost the same hydrographic properties of OYW with lower DFe concentrations (< 0.26 nM) at each station (Table 1). At Stn. A4–4 of OYW in May, macronutrient concentrations were equivalent to those at Stn. A5 during OECOS in April, but Chl a and DFe concentrations were low. At Stns. B3–4 and B3–5 of OYW in May, macronutrient levels were relatively high, but DFe concentrations were low.

Phytoplankton assemblages based on HPLC-CHEMTAX analysis

Our HPLC–CHEMTAX results (Fig. 4) showed that diatoms were the major phytoplankton group during OECOS. Contributions of cryptophytes to the Chl a biomass during OECOS were relatively high (ca. 10%) at both the surface and 5% OD in 16 April–19 April and 29 April to 01 May when the station was occupied by the MKW. Dinoflagellates tended to increase gradually over time during OECOS. Phytoplankton compositions during BLOSSOM differed from those during OECOS (Fig. 4). Although diatoms were widely distributed at Stns. B1

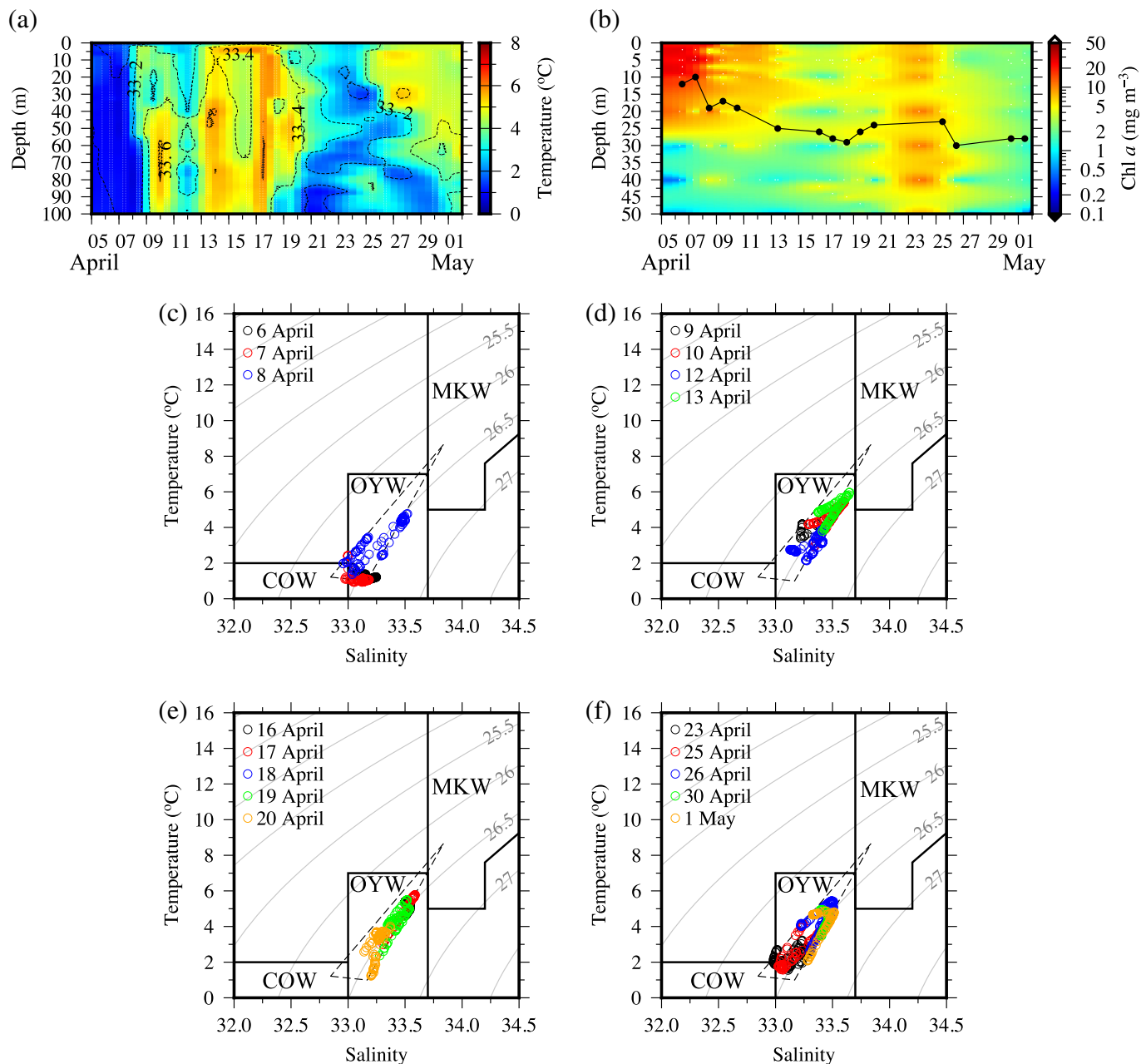


Fig. 2. Temporal changes in (a) the vertical profiles of temperature and salinity measured by CTD and (b) the vertical profiles of Chl *a* concentrations measured by fluorometry and the euphotic layer depth (Z_{eu}) at Stn. A5 during the OECOS cruise from 05 April to 01 May 2007. Dashed lines in (a) and black symbols in (b) represent salinity in intervals of 0.2 and Z_{eu} , respectively. (c–f) Temperature–salinity diagrams from the surface to 100 m depth at Stn. A5 during the OECOS cruise. Triangles with dashed line represent the definition area of the mixing ratio analysis using three water mass (OYW, Oyashio water; COW, Coastal Oyashio water, and MKW, modified Kuroshio Water) proposed by Kono and Sato (2010).

and B2 of a consistent water mass of OYW at both the surface and 5% OD in May (i.e., Stns. B1-4, B1-5, B2-4, and B2-5), the contributions to Chl *a* biomass of phytoplankton groups other than diatoms increased at the surface in June. As revealed from the pigment signatures, cyanobacteria occurred at all stations observed in June regardless of different water masses (i.e., Stns. B1-6, B1-7, B2-6, B2-7, and A4-6).

Abundance and diversity of diatoms

At least 85 diatom species were identified by SEM in this study (Table 2). Centric diatoms were predominant in this study, compared with pennate diatoms (Fig. 5a,b). Higher cell abundance was measured from 06 April 2007 to 08 April 2007 and 12 April 2007 at Stn. A5 during OECOS, when the COW occupied the water mass. The sum of *Thalassiosira anguste-*

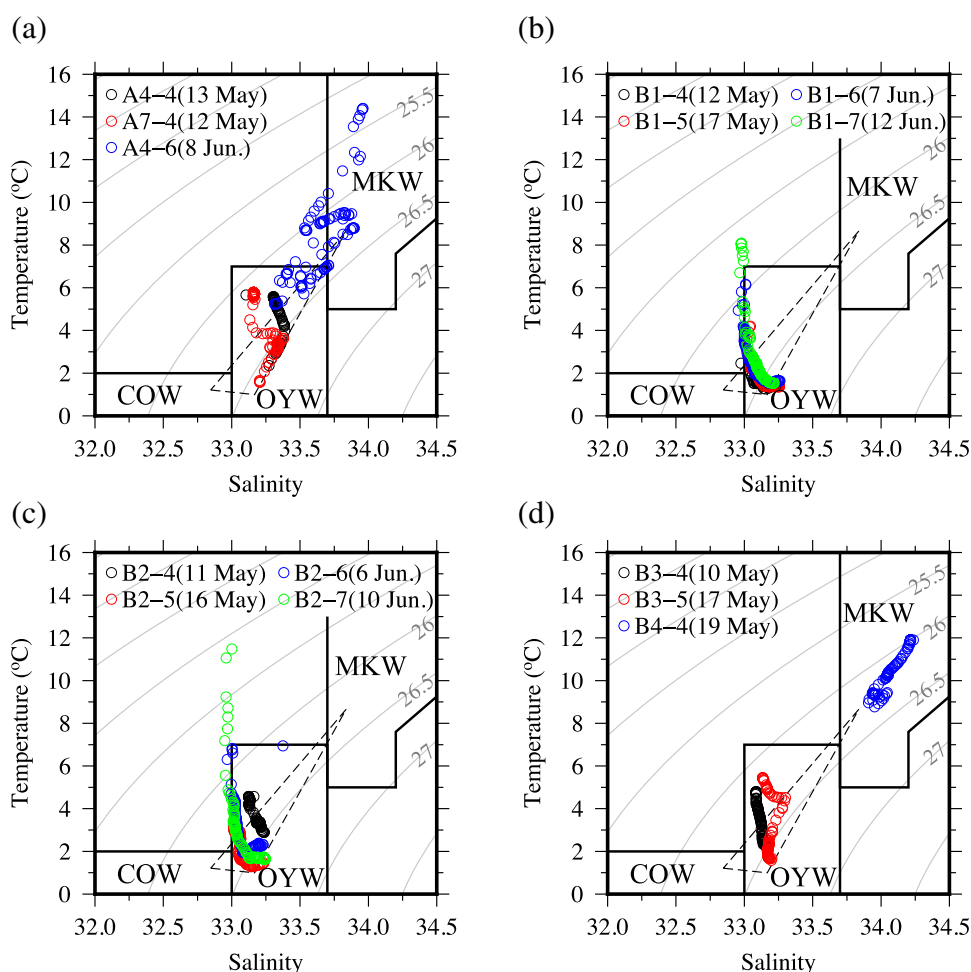


Fig. 3. Temperature–salinity diagrams at Stns. (a) both A4 and A7, (b) B1, (c) B2, and (d) both B3 and B4 during the BLOSSOM cruises in May and June 2007. Triangles are as in Fig. 2.

lineata, *T. hyalina*, *T. nordenskiöldii*, *T. pacifica*, and *Thalassiosira* spp. abundance accounted for ca. 40% of the total diatoms during OECOS (Fig. 6a). Similarly, the relative abundances of summed *Chaetoceros compressus*, *C. debilis*, *C. diadema*, *C. radicans*, and *Chaetoceros* spp. accounted for another ca. 40% of the total diatoms during OECOS. However, the contribution of *C. radicans* to the total diatom abundance was > 46% from 25 April to 01 May. The relative abundance of *Fragilariopsis* spp. was somewhat enhanced in the MKW-dominated waters in 13 April and 17 April. Throughout the OECOS cruise, total diatom abundance and cell densities of *C. diadema* and *T. nordenskiöldii* were positively correlated with the composition of COW to the observed water masses and negatively correlated with both MLD and the composition of MKW to the observed water masses (Table 3).

During BLOSSOM, abundance and composition of diatom species dramatically varied spatially and temporally (Fig. 5b). At Stns. B1 and B2 of a consistent water mass of OYW, diatom cell abundance was relatively low in the first half of May (Table 1). However, after 5 d of observations at these sites,

diatom abundance increased. Especially, the contribution of *Thalassiosira* species to the total diatoms increased with values reaching values similar to those in the beginning of OECOS cruise. After that, higher abundances of diatoms were found at these stations in June (Stns. B1-7 and B2-7). The values were comparable to or higher than those observed in 06 April–08 April of the OECOS cruise, but the compositions of diatoms between April and June were clearly distinct. *C. debilis* was predominant among the diatom community at these stations in June (Fig. 6b). Generally, *Chaetoceros* species became predominant at other stations of OYW (Stns. A4-4, A7-4, B3-4, and B3-5) and at Stn. A4-7 and B4-4 of MKW (Fig. 6b).

Values of H' for the diatoms species tended to decrease over time during OECOS (Fig. 5c). Lower values were found in the end of the cruise where the diatoms mainly consisted of *C. radicans*. During BLOSSOM, the index values varied, ranging from 0.8 to 2.6 (Fig. 5d). The values were low especially at Stns. A7-4, B2-7 and B3-5 of OYW and at Stns. A4-6 and B4-4 of MKW where *C. radicans* and/or *C. debilis* principally dominated diatoms abundance.

Table 1. Summary of hydrographic data, Chl *a* concentration measured by fluorescence, mixing ratios of OYW, COW, and MKW to the observed water masses during OECOS, and water mass classification based on Hanawa and Mitsudera (1987) during BLOSSOM at 5 m depth. Note that mixing ratios during OECOS were calculated with the data at 10 m depth to avoid the spikes of the CTD data above the depth following Kono and Sato (2010) and dissolved iron (DFe) concentrations during the BLOSSOM cruise were obtained from 10 m depth. Temp, temperature; MLD, mixed layer depth; Z_{eu} , the euphotic layer depth; daily PAR, daily photosynthetically available radiation; $NO_3 + NO_2$, nitrite + nitrate; PO_4 , phosphate; $Si(OH)_4$, silicate; Chl *a*, chlorophyll *a* concentration; OYW, Oyashio water; COW, coastal Oyashio water; MKW, modified Kuroshio water.

Date	Temp (°C)	Salinity	MLD (m)	Z_{eu} (m)	Daily PAR (mol photons $m^{-2} d^{-1}$)	$NO_3 + NO_2$ (μM)	PO_4 (μM)	$Si(OH)_4$ (μM)	DFe (nM)	Chl <i>a</i> (mg m^{-3})	OYW (%)	COW (%)	MKW (%)
OECOS (A5)													
06 April	1.7	33.03	44	12	43.0	8.92	0.69	19.03	0.44	19.85	35.5	56.5	7.9
07 April	2.2	33.00	24	10	31.7	2.04	0.26	5.08	0.44	19.85	0.0	83.9	16.1
08 April	2.0	32.96	46	19	34.1	2.12	0.29	2.45	0.53	18.85	10.0	78.2	11.8
09 April	4.1	33.23	34	17	41.5	5.47	0.82	5.14	-	2.64	0.0	60.1	39.9
10 April	4.2	33.31	88	19	44.0	5.71	0.35	3.87	0.38	4.65	14.9	44.8	40.3
12 April	2.8	33.14	62	-	28.3	13.19	0.80	18.68	0.22	8.18	14.8	57.4	27.8
13 April	4.9	33.38	81	25	40.3	4.99	0.25	1.96	0.29	3.50	12.3	38.1	49.5
16 April	5.4	33.50	137	26	43.6	8.67	0.46	9.78	0.26	1.76	27.6	15.4	57.0
17 April	5.9	33.61	127	28	40.7	10.45	0.55	14.45	0.20	1.55	37.5	1.1	61.5
18 April	5.6	33.54	104	29	48.9	8.85	0.42	10.26	0.47	3.18	32.8	6.9	60.3
19 April	5.5	33.51	103	26	49.8	8.79	0.40	9.53	0.19	2.27	29.1	12.6	58.3
20 April	3.6	33.24	82	24	36.2	9.95	0.53	11.00	0.18	3.91	21.5	44.8	33.7
23 April	2.6	33.01	49	-	32.1	4.15	0.30	5.11	0.35	9.26	0.0	80.9	19.1
25 April	4.0	33.22	67	23	12.9	7.48	0.40	5.35	0.26	3.83	3.2	58.2	38.6
26 April	4.2	33.23	65	30	45.1	6.72	0.33	3.47	0.24	2.50	0.0	61.7	38.3
30 April	4.9	33.38	76	28	53.5	10.42	0.55	10.69	0.26	2.30	15.5	34.4	50.1
01 May	4.6	33.31	60	28	41.2	9.86	0.53	8.43	0.17	2.28	6.5	46.9	46.6
Station (Date)	Temp (°C)	Salinity	MLD (m)	Z_{eu} (m)	Daily PAR (mol photons $m^{-2} d^{-1}$)	$NO_3 + NO_2$ (μM)	PO_4 (μM)	$Si(OH)_4$ (μM)	DFe (nM)	Chl <i>a</i> (mg m^{-3})	Water mass classification		
BLOSSOM2&3													
A4-4 (13 May)	5.7	33.105	76	42	24.7	9.9	1.03	8.0	0.20	0.90	OYW		
A4-6 (08 June)	14.4	33.959	10	45	39.0	0.1	0.16	0.7	0.11	0.78	MKW		
A7-4 (12 May)	5.8	33.157	57	27	25.0	4.1	0.62	4.0	0.44	4.84	OYW		
B1-4 (12 May)	2.5	33.060	70	43	25.0	23.3	1.93	44.8	0.26	1.20	OYW		
B1-5 (17 May)	4.2	33.044	62	45	19.2	19.1	1.61	42.2	0.26	7.44	OYW		
B1-6 (7 June)	6.1	33.011	14	21	36.4	18.0	1.59	37.7	0.15	2.82	OYW		
B1-7 (12 June)	8.1	32.980	12	20	42.3	5.0	0.62	12.4	0.12	9.41	OYW		
B2-4 (11 May)	4.6	33.163	36	25	10.3	19.3	1.67	36.3	0.16	1.82	OYW		
B2-5 (16 May)	3.6	33.031	53	42	34.6	19.6	1.71	43.1	0.16	7.00	OYW		
B2-6 (6 June)	7.0	33.375	20	38	52.9	19.3	1.71	39.1	0.20	0.95	OYW		
B2-7 (12 June)	11.5	33.001	11	-	42.3	10.0	0.89	21.5	0.08	5.51	OYW		
B3-4 (10 May)	4.8	33.395	44	47	12.0	20.2	1.73	38.7	0.17	1.06	OYW		
B3-5 (17 May)	5.5	32.313	37	27	19.2	14.0	1.17	19.0	0.09	2.93	OYW		
B4-4 (19 May)	11.9	33.308	44	35	11.3	4.9	0.45	9.6	0.12	2.67	MKW		

Table 2. List of diatom species identified by SEM at 5 m during the OECOS and BLOSSOM cruises.

Centric diatoms		Pennate diatoms	
<i>Actinoptychus senarius</i>	<i>C. simplex</i>	<i>Skeletonema costatum</i>	<i>Cylindrotheca closterium</i>
<i>Asteromphalus elegans</i>	<i>C. socialis</i>	<i>Stephanopixis nipponica</i>	<i>Fragilariopsis atlantica</i>
<i>A. flabellatus</i>	<i>C. tenuissimus</i>	<i>Stephanopyxis turris</i>	<i>F. antarctica</i>
<i>A. hookeri</i>	<i>Chaetoceros</i> spp.	<i>Thalassiosira allenii</i>	<i>F. cylindrus</i>
<i>A. hyalms</i>	<i>Corethron criophilum</i>	<i>T. anguste-lineata</i>	<i>F. oceanica</i>
<i>Bacteriosira bathyomphala</i>	<i>Coscinodiscus alboranii</i>	<i>T. antarctica v. borealis</i>	<i>Fragilariopsis</i> spp.
<i>Bacteriastrium comosum</i>	<i>Cos. Granii</i>	<i>T. eccentrica</i>	<i>Nitzschia distans</i>
<i>B. delicatulum</i>	<i>Cos. Gigas</i>	<i>T. gracilis</i>	<i>N. pelagica</i>
<i>B. hyalinum</i>	<i>Dactyliosolen fragilissimus</i>	<i>T. gravida</i>	<i>Nitzschia</i> spp.
<i>Chaetoceros atlanticus</i>	<i>Eucampia zodiacus</i>	<i>T. hyalina</i>	<i>Navicula</i> spp.
<i>C. compressus</i>	<i>Eucampia</i> sp.	<i>T. kushirensis</i>	<i>Neodelphineis pelagica</i>
<i>C. concavicornis</i>	<i>Hemiaulus hauckii</i>	<i>T. lineata</i>	<i>Neodenticula seminae</i>
<i>C. convolutus</i>	<i>Lauderia annulata</i>	<i>T. nordenskiöldii</i>	<i>Pseudo-nitzschia delicatissima</i>
<i>C. curvisetus</i>	<i>Leptocylindrus</i> sp.	<i>T. osteropii</i>	<i>Pseudo-nitzschia granii</i>
<i>C. debilis</i>	<i>Minidiscus comicus</i>	<i>T. pacifica</i>	<i>Pseudo-nitzschia seriatu</i>
<i>C. decipiens</i>	<i>Odontella aurita</i>	<i>T. rotula</i>	<i>Pseudo-nitzschia</i> spp.
<i>C. diadema</i>	<i>Proboscia alata</i>	<i>T. trifulta</i>	<i>Thalassiothrix longissima</i>
<i>C. dydimus</i>	<i>Prosira gracilis</i>	<i>Thalassiosira</i> spp.	<i>Thalassionema nitzschioides</i>
<i>C. furcellatus</i>	<i>Prosira pentaportula</i>		<i>Thalassionema pseudonitzschioides</i>
<i>C. laciniosus</i>	<i>Rhizosolenia hebetata</i>		<i>Thalassionema</i> sp.
<i>C. neglectus</i>	<i>R. hebetata, semispia</i>		
<i>C. radicans</i>	<i>R. acicularis</i>		
<i>C. pseudocurvisetus</i>	<i>Rhizosolenia</i> sp.		
<i>C. similis</i>			

Cluster analysis (Fig. 7a) based on the diatom species observed by SEM mainly classified the data set into the OECOS and BLOSSOM groups. Of the OECOS cruise, data obtained in 06 April–08 April and 12 April was categorized into the same group. Data at Stns. B1-5 and B2-5 of OYW in the middle of May during BLOSSOM were grouped with the OECOS cluster because of the predominance of *Thalassiosira* species. In the Redundancy analysis (RDA) for investigating relationships between the abundance of each diatom species

and environmental factors (Fig. 7b), the first and second axes explained 45% and 16% of the variation, respectively. Temperature and DFe concentrations were the main environmental factors contributing to the formation of the first axis. The second axis was mainly affected by MLD and salinity. During OECOS, the diatom community was mainly affected by water masses with lower temperatures and higher DFe concentrations, especially in 06 April–08 April and 12 April, corresponding with the high contribution of COW to the observed water

Table 3. Kendall rank correlations coefficients (τ) between the contributions of OYW, COW, and MKW to the observed water masses as well as MLD and Chl *a* concentration, total cell density of diatoms, cell concentrations of the major diatom species described in Fig. 6a during the OECOS cruise.

	Chl <i>a</i>	Total cell density	<i>C. compressus</i>	<i>C. debilis</i>	<i>C. diadema</i>	<i>C. radicans</i>	<i>T. anguste lineata</i>	<i>T. hyalina</i>	<i>T. nordenskiöldii</i>	<i>T. pacifica</i>
OYW	−0.31	−0.31	−0.08	−0.28	−0.46	−0.40	0.01	−0.05	−0.27	−0.03
	0.25	0.24	0.78	0.29	0.07	0.13	0.98	0.85	0.31	0.90
COW	0.59	0.57	0.42	0.49	0.71	0.50	0.22	0.31	0.56	0.33
	$p < 0.05$	$p < 0.05$	0.10	0.06	$p < 0.01$	$p < 0.05$	0.42	0.24	$p < 0.05$	0.22
MKW	−0.76	−0.65	−0.62	−0.52	−0.73	−0.45	−0.33	−0.44	−0.76	−0.44
	$p < 0.001$	$p < 0.01$	$p < 0.05$	$p < 0.05$	$p < 0.01$	0.08	0.21	0.09	$p < 0.001$	0.09
MLD	−0.59	−0.60	−0.60	−0.55	−0.68	−0.53	−0.22	−0.39	−0.61	−0.33
	$p < 0.05$	$p < 0.05$	$p < 0.05$	$p < 0.05$	$p < 0.01$	$p < 0.05$	0.21	0.09	$p < 0.05$	0.09

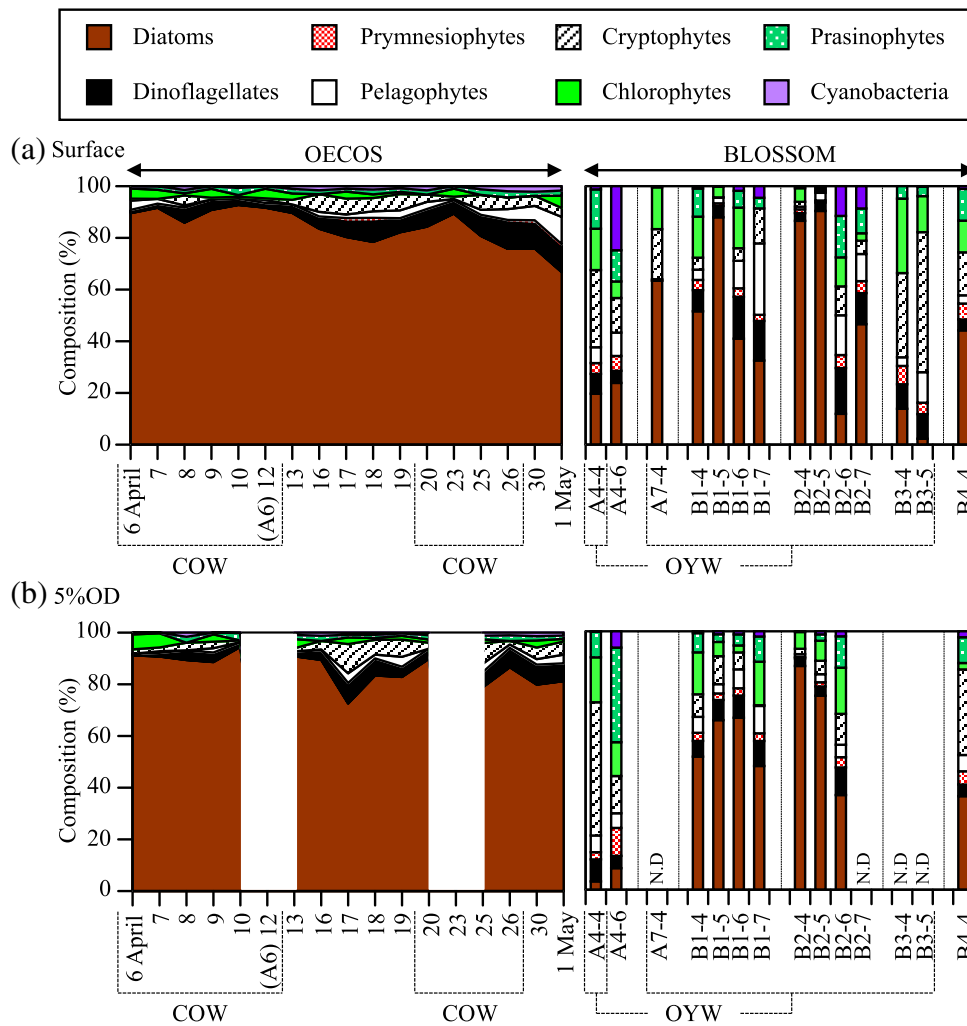


Fig. 4. Composition of each phytoplankton group to Chl *a* concentration as estimated by HPLC-CHEMTAX analysis at (a) the surface and (b) 5% optical depth (OD). Note that samples at Stns. A4-7, B2-7, B3-4, and B3-5 were taken from 10 m depth. COW and OYW with dashed lines in the x-axis indicate the COW- and OYW dominant waters during the OECOS and BLOSSOM cruises, respectively. Blanks represent the MKW-dominated waters.

masses. The rest of OECOS data were associated with higher MLD and salinity. In contrast, the diatom assemblages observed in the BLOSSOM cruises were not ordinated close to the DFe vector.

Fd and Fld accumulation in micro-sized diatoms and F_v/F_m in micro-sized phytoplankton

Ferredoxin (Fd, an iron-containing photosynthetic protein) in micro-sized diatoms was not detected during both OECOS and BLOSSOM cruises. Rather, flavodoxin (Fld, iron-free protein) was detected in these diatoms throughout the study period except for the observations at Stns. A4-4 and A7-4 of OYW in May (Fig. 8). Accumulation of Fld was high especially in the middle of May (Stn. B1-5 and B2-5). A remarkable decline in F_v/F_m of the micro-sized phytoplankton community (F_v/F_{m_Micro}) was found from 06 April to 10 April during OECOS. Then, the values of F_v/F_{m_Micro} fluctuated until

20 April and were consistently high after 23 April. During the BLOSSOM cruises in May and June, higher F_v/F_{m_Micro} values were found at Stns. B1 and B2 of a consistent water mass of OYW in May (i.e., Stns. B1-4, B1-5, B2-4, and B2-5). Kendall rank correlation coefficients using all data sets and the data set of each cruise showed no significant relationship between Fld and F_v/F_{m_Micro} and that none of the environmental variables (temperature, salinity, macro-nutrients, and DFe) were statistically correlated to Fld or F_v/F_{m_Micro} .

PE parameters

Values of P^B_{max} and α^B showed approximately fourfold and sixfold variations throughout the field campaigns, respectively (Fig. 9a,b,e,f). During OECOS, the parallel changes in P^B_{max} and α^B were found at both the surface ($R = 0.71$, $p < 0.01$, $n = 15$) and 5% OD ($R = 0.84$, $p < 0.001$, $n = 13$). As a result, the variations in E_k at both depths were constant (surface;

115 ± 31 μmol photons m⁻² s⁻¹, 5%LD; 77 ± 13 μmol photons m⁻² s⁻¹), indicating E_k -independent variability of PE parameters (Behrenfeld et al. 2008; Milligan et al. 2015). The changes in P_{\max}^B and E_k showed a typical pattern of higher P_{\max}^B and E_k values at the surface than those at 5% OD due to photoacclimation (Wilcoxon signed rank test: P_{\max}^B , $p < 0.01$, $n = 23$; E_k , $p < 0.001$, $n = 23$). The values of F_v/F_m for the overall phytoplankton assemblage and Φ_{\max} at the surface also varied widely (Fig. 9c,d,g,h). The values of Φ_{\max} were high in 07 April and 12 April during OECOS and at Stns. B1-4 and B2-4 in May during BLOSSOM. The lower F_v/F_m and Φ_{\max} values at the surface than at 5% OD were found during the OECOS cruise (Wilcoxon signed rank test: F_v/F_m , $p < 0.05$, $n = 13$; Φ_{\max} , $p < 0.01$, $n = 13$). However, the differences in F_v/F_m and Φ_{\max} between the surface and 5% OD were not statistically significant during the BLOSSOM cruises. Kendall rank correlation coefficients showed significant relationships between F_v/F_m and temperature or salinity at the surface (temperature; $\tau = -0.65$, $p < 0.01$, $n = 16$, salinity; $\tau = -0.53$, $p < 0.05$, $n = 16$) during OECOS. Consequently, the values of F_v/F_m were positively and negatively correlated with the mixing ratios of COW ($\tau = 0.57$, $p < 0.05$, $n = 16$) and MKW ($\tau = -0.60$, $p < 0.05$, $n = 16$) during OECOS, respectively. Other photosynthetic parameters during OECOS were not significantly correlated with the environmental variables and mixing ratios. During BLOSSOM, a significant relationship between Φ_{\max} and temperature at the surface ($\tau = -0.64$, $p < 0.05$, $n = 10$) was found. Variations in F_v/F_m and Φ_{\max} as well as \bar{a}_{ph}^* were significantly correlated with temperature throughout the whole observations (F_v/F_m ; $\tau = -0.50$, $p < 0.01$, $n = 26$, Φ_{\max} ; $\tau = -0.58$, $p < 0.01$, $n = 25$, \bar{a}_{ph}^* ; $\tau = 0.56$, $p < 0.01$, $n = 25$).

Discussion

Diatom community and Fe stress of large diatoms during the spring bloom in the Oyashio region

Massive spring blooms (> 5 mg m⁻³ in Chl a biomass) were found at Stn. A5 in April 2007 during the Eularian survey of OECOS and at Stns. B1 and B2 from the middle of May to June 2007 during spatiotemporal monitoring through the BLOSSOM cruises. Our CHEMTAX results showed that diatoms were the major constituent of the populations throughout our study period. The diatom species identified by SEM consisted of a mixture of *Thalassiosira* and *Chaetoceros* species. Previous studies also showed that these species were co-dominant during the spring bloom in the Oyashio region (Chiba et al. 2004; Tsuda et al. 2005; Hattori-Saito et al. 2010; Suzuki et al. 2011; Nosaka et al. 2017). However, our high-frequency observations revealed diatom taxa succession from *Thalassiosira* spp. or a mixture of *Thalassiosira* and *Chaetoceros* spp. to dominance by *Chaetoceros* spp. during both the OECOS and BLOSSOM cruises from April to June 2007 (Fig. 6). Shannon-Wiener index values for diatom taxa clearly

decreased from 25 April to 01 May during OECOS and were relatively low at Stns. A4-6, A7-4, B2-7, B3-5, and B4-4 during BLOSSOM (Fig. 5c,d). A common characteristic of these stations was that *Chaetoceros radicans* and/or *Chaetoceros debilis* were predominant among diatoms.

The relative abundance of cryptophytes and cyanobacteria to the total phytoplankton increased post bloom, which is consistent with previous studies based on CHEMTAX analysis (Isada et al. 2009; Suzuki et al. 2011). During OECOS, contribution of cryptophytes to the Chl a levels as estimated with CHEMTAX were relatively high in high proportion of MKW (Fig. 4), which was in good agreement with the cell abundance of cryptophytes measured by flow cytometry from data taken during OECOS (Sato and Furuya 2010).

Our extensive observations with an immunological Fd/Fld assay showed flavodoxin accumulation without ferredoxin detection throughout the spring bloom from April to June 2007 in all water masses observed in this study. Mesoscale iron fertilization experiments in the eastern (SERIES) and western (SEEDS II) subarctic Pacific also showed that only flavodoxin was detected even after iron additions (Boyd et al. 2005; Suzuki et al. 2009). Previous studies both in the field (La Roche et al. 1996) and in laboratory experiments with cultures (McKay et al. 1997; Davey and Geider 2001; Whitney et al. 2011) demonstrate that Fld is expressed as an early-stage response to Fe stress. Boyd et al. (1999) showed that the Fld accumulation was remarkably alleviated at > ca. 1 nM DFe concentration. During OECOS, although water masses affected by the COW have higher DFe concentrations (Table 1) and macro-nutrients were not depleted, DFe concentrations did not exceed 0.53 nM. Nishioka et al. (2011) showed that the COW during the winter season had higher DFe concentration (up to 2.8 nM) compared with the OYW and MKW. Additionally, Hattori-Saito et al. (2010) showed the accumulation of Fd in micro-sized diatoms under high DFe concentration (6.37 nM) at Stn. A4 before the spring bloom in 2005. Therefore, our results suggested that the growth of micro-sized diatoms might be iron limited during spring bloom in the Oyashio region. However, Marchetti et al. (2012) showed based on comparative metatranscriptomics for identifying iron-activated gene expression of diatoms at Ocean Station Papa in the NE Pacific Ocean that transcription linked with Fld gene expression were abundant in all libraries even after iron addition, indicating that some or all diatoms continued to use Fld for the photosynthetic electron transport (PET) chain rather than transitioning fully to Fd. They suggested that chronically iron-limited diatom communities do not use ferredoxin or may have lost the gene for ferredoxin to adapt to low Fe conditions. Additionally, Carradec et al. (2018) investigated eukaryotic genes in the world ocean and found a more constitutive expression of Fld for diatoms under all iron conditions, suggesting that in contrast to other phytoplankton groups (e.g., chlorophytes, haptophytes, and pelagophytes) with the flexible switching strategy of Fd/Fld, diatoms

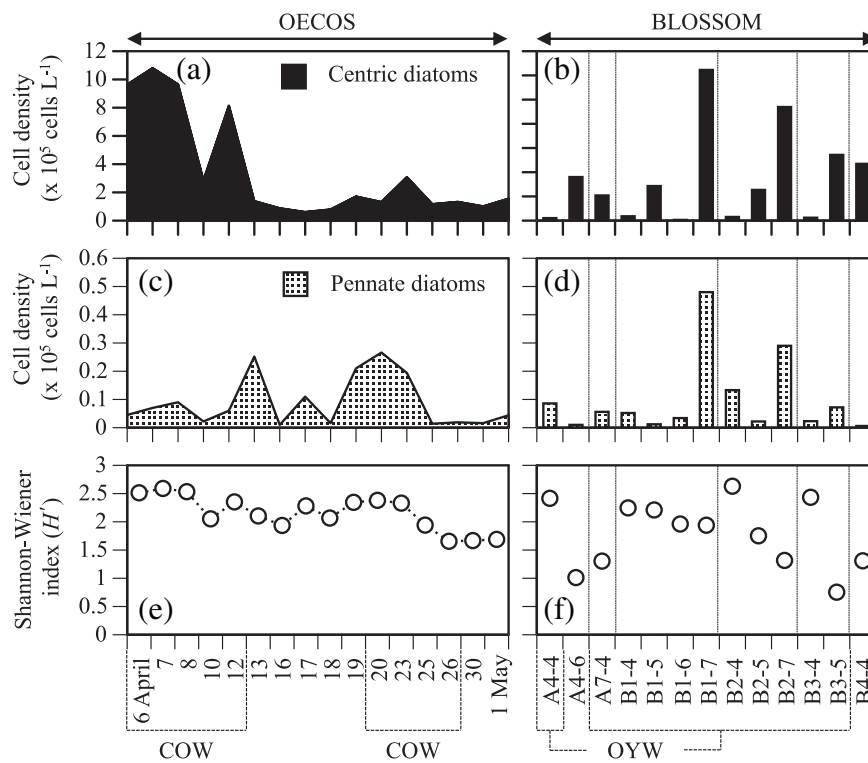


Fig. 5. Changes in cell density of (a, b) centric and (c, d) pennate diatoms measured by a scanning electron microscope (SEM) and (e, f) Shannon Wiener index (H') during the OECOS and BLOSSOM cruises. COW and OYW with dashed lines are as in Fig. 4.

may be permanently adapted to use Fld. More information is needed to evaluate whether micro-sized diatoms were stressed or limited by iron deficiency in the Oyashio region.

Although significant relationships between Fld and both photosynthetic parameters and environmental variables were not found in this study, F_v/F_m and Φ_{cmax} gradually decreased toward the end of the OECOS cruise (Fig. 9c,g), despite hydrography showing that macro-nutrients were not depleted. The decreases in F_v/F_m under macronutrient-replete, but possibly iron limiting conditions during OECOS may be a consequence of disconnected light-harvesting complexes (DLHCs) acting in a photoprotective manner (Behrenfeld et al. 2006; Behrenfeld and Milligan 2013). The DLHCs contain chlorophyll but are functionally disconnected from PSII, so that the presence of these complexes should decrease apparent assimilation efficiencies in measurements of productivity. The DLHCs effect is expressed through E_k -independent variability of PE parameters (Behrenfeld and Milligan 2013). Accordingly, our E_k -independent variability observed during OECOS (see "PE parameters" section) could be a consequence of iron stress in the phytoplankton community. Similarly, previous studies (Isada et al. 2009; Yoshie et al. 2010) showed E_k -independent variability during the spring bloom in the Oyashio region. It is known that the variability is accompanied by the allocation of adenosine triphosphate (ATP) and nicotinamide adenine dinucleotide phosphate (NADPH) made by PET chain in a coordinated fashion to regulate the supply of photosynthate to the

Calvin-Benson cycle (Behrenfeld et al. 2008; Halsey et al. 2010). Therefore, our results showing E_k -independent variability during OECOS were consistent with an acclimation strategy of diatoms for iron deficiency during the spring bloom in the Oyashio region. However, E_k -independent behavior does not necessarily result from DLHCs only. The variability is largely affected by growth rate (Halsey et al. 2010). Therefore, further study for evaluating iron-stress of diatoms during spring bloom in the Oyashio region is required.

The abundances of Fld during BLOSSOM were highly variable. Low or zero Fld values at Stn. A4-4 of OYW and at Stn. A4-6 and A7-4 of MKW could be related with the cross-reactivity of the antibodies among diatom species (Hattori-Saito et al. 2010). Pico- and nano-sized phytoplankton groups were predominant at Stn. A4 during BLOSSOM (Isada et al. 2010). Our CHEMTAX results (Fig. 4) also showed higher contributions of phytoplankton other than diatoms to the Chl *a* biomass during BLOSSOM. The abundances of Fld at Stns. B1 and B2 of a consistent water mass of OYW (Figs. 3, 8) from May to June 2007 were highly variable under low DFE conditions (< 0.26 nM), but a strong significant relationship between F_v/F_m and Φ_{cmax} at the surface was identified (Fig. 10). These results indicated that the phytoplankton assemblages regulated photosynthesis for acclimating to changing environmental conditions as the bloom progressed, possibly by changing allocation of electron flow to maintain

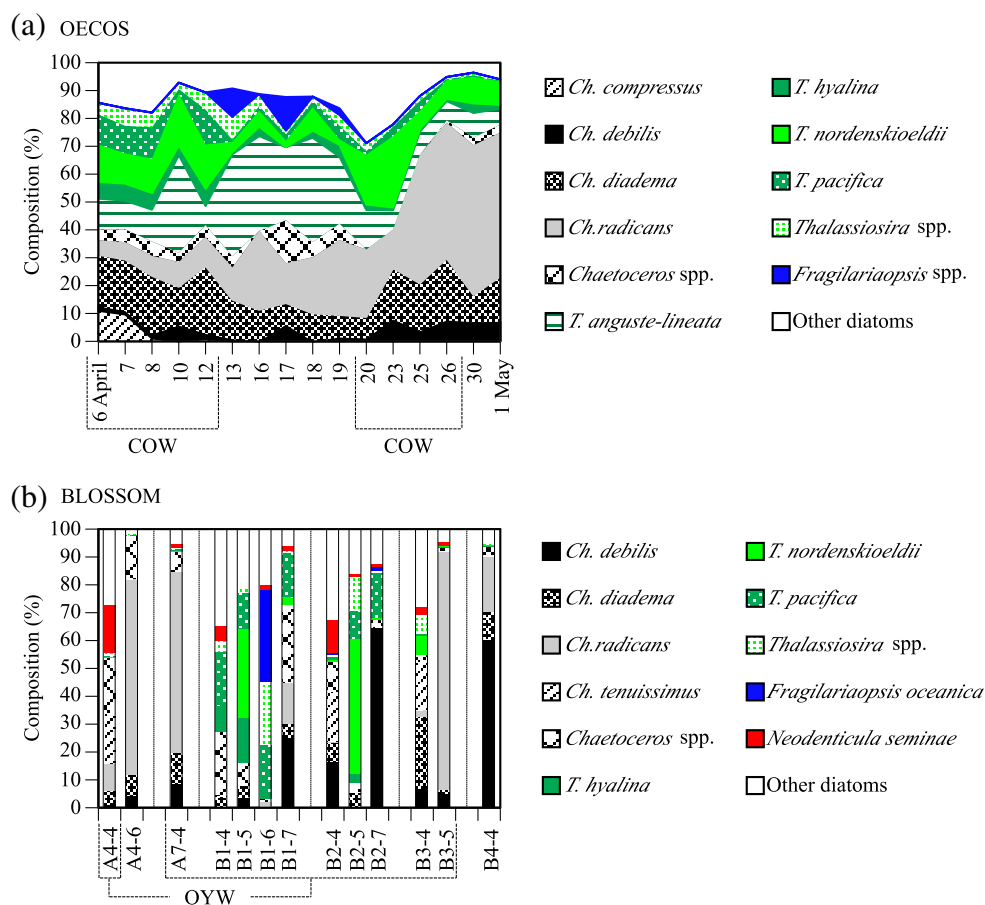


Fig. 6. Composition of major diatom species measured by SEM to total diatom cell density during the (a) OECOS and (b) BLOSSOM cruises. COW and OYW with dashed lines are as in Fig. 4.

optimal photosynthetic performance (Halsey et al. 2013; Lawrenz et al. 2013; Halsey and Jones 2015).

Spatial heterogeneity of the spring bloom in the Oyashio region

Our high frequency sea observations also revealed spatio-temporal heterogeneity of the spring diatom bloom in the Oyashio region during 2007 (Table 1; Fig. 1). Although massive spring diatom blooms were found at Stn. A5 especially in early April 2007, diatom blooms at Stns. B1 and B2 of OYW in the eastern part of Oyashio region had not initiated until the middle of May 2007. Generally, the spring bloom occurred from April to May guided by the water-column stratification, but magnitude and timing of the bloom varies from year to year (Kasai et al. 1997; Saito et al. 2002; Okamoto et al. 2010; Shiozaki et al. 2014).

Water properties at Stn. A5 during OECOS were highly complex owing to varying contributions of COW, OYW, and MKW (Table 1; Fig. 2, Kono and Sato 2010). We found that Chl *a* concentration, total cell density of diatoms, and the abundances of *T. nordenskiöldii* and *C. diadema* were positively and negatively correlated with the contribution of

COW and MKW to the observed water masses, respectively (Table 3). Of the photosynthetic parameters we measured in this study, F_v/F_m values for the total phytoplankton assemblages were positively and negatively correlated with the relative composition of COW and MKW, respectively (see “PE parameters” section). Shinada et al. (1999a,b) showed the predominance of *Thalassiosira* spp. at the beginning of the spring bloom in COW. Therefore, our results suggested that the magnitude of the spring bloom in the Oyashio region in “April” was strongly affected by intrusion of COW into offshore region of the Oyashio region and was potentially diluted by MKW. In fact, the distribution of the composite image of Chl *a* concentration derived from MODIS/Aqua during 05 April 2007–11 April 2007 (Fig. 1) showed a southbound water mass and elongated filaments with high Chl *a* level. Okamoto et al. (2010) also showed, using 10-yr satellite ocean color and altimeter data from 1998 to 2007, the southbound coastal water having high Chl *a* concentration along the edges associated with mesoscale eddies. The sub-mesoscale processes can affect physical and chemical dynamics (e.g., the intensity of mixed layer depth, formation of fronts, and advection of nutrients from the bottom), thereby influencing the

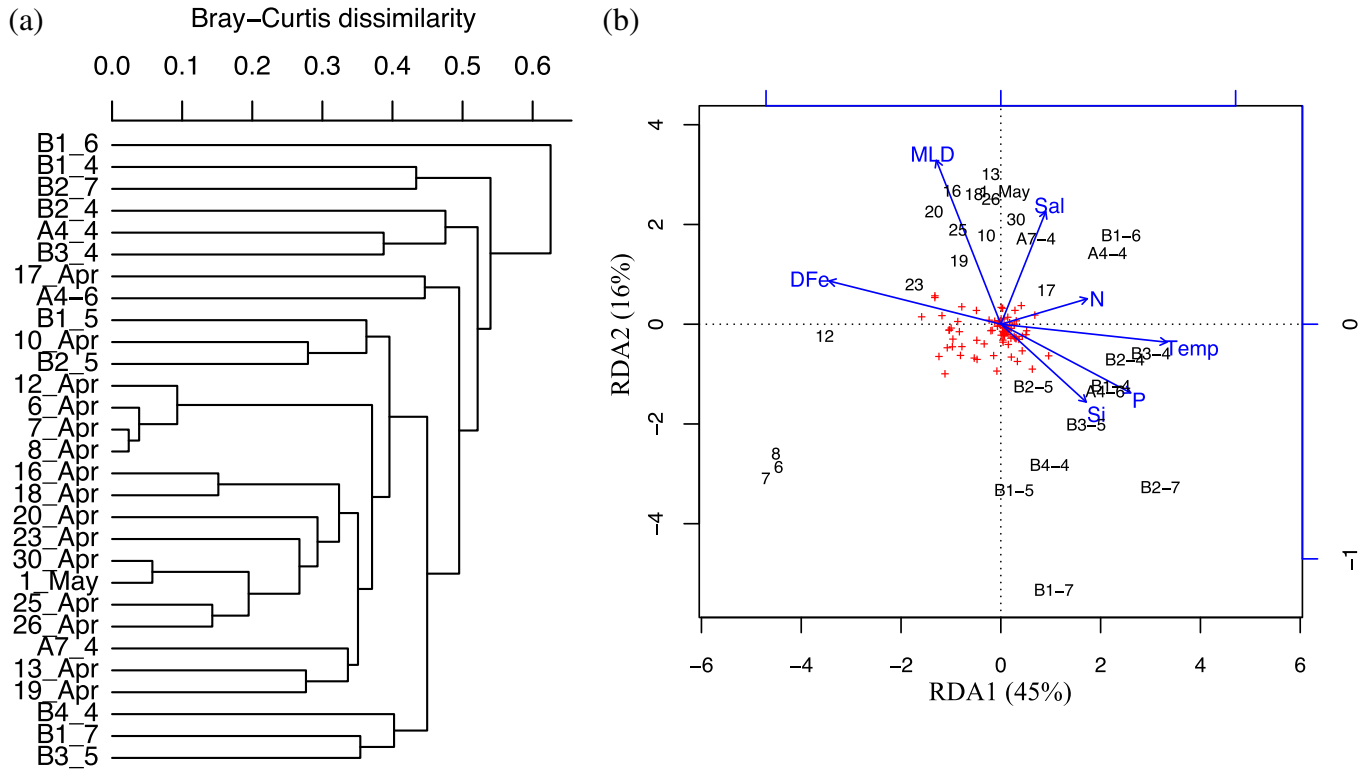


Fig. 7. (a) Result of cluster analysis with Bary-Curtis dissimilarity and UPGMA based on diatom species measured by SEM and (b) redundancy analysis (RDA) ordination diagram relative to cell density of diatom species measured by SEM at the surface. Arrows in (b) refer to environmental variables (temp, sea temperature; Sal, salinity; N, nitrate; P, phosphate; Si, silicate; DFe, dissolved iron, MLD; mixed layer depth). Numbers in (b) represent days in April 2007 during the OECOS cruise.

patchiness of Chl *a* distribution and phytoplankton productivity (Falkowski et al. 1991; Gruber et al. 2011; Mahadevan 2016). Additionally, we found the negative correlations between MLD and Chl *a* concentration, total cell density of diatoms, and the abundances of *T. nordenskioldii* and *C. diadema* (Table 3). RDA results (Fig. 7b) also showed that MLD was associated with the OECOS diatom species composition except for the water masses strongly affected by COW

(6, 7, 8, 12, and 23 April). Therefore, our results also suggested that the elongated COW having higher Chl *a* concentrations associated with mesoscale eddies was diluted by an encounter with MKW having the deep MLD.

While the massive diatom bloom accompanied by COW dynamics occurred at Stn. A5 in April 2007, intensive blooms at Stns. B1 and B2 of OYW in the eastern part of the Oyashio region were not found until the middle of May 2007. Our

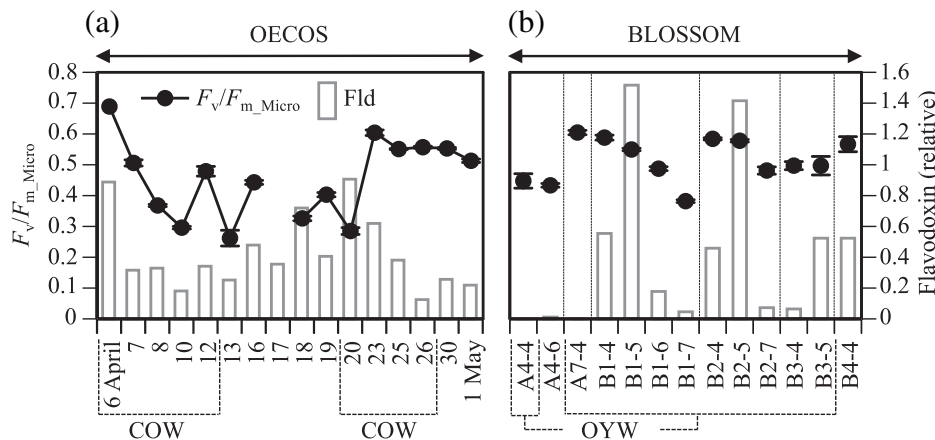


Fig. 8. Changes in F_v/F_m of micro-sized phytoplankton and abundances of flavodoxin (Fld) of micro-sized diatoms at ca. 5 m depth during the (a) OECOS and (b) BLOSSOM cruises. COW and OYW with dashed lines are as in Fig. 4.

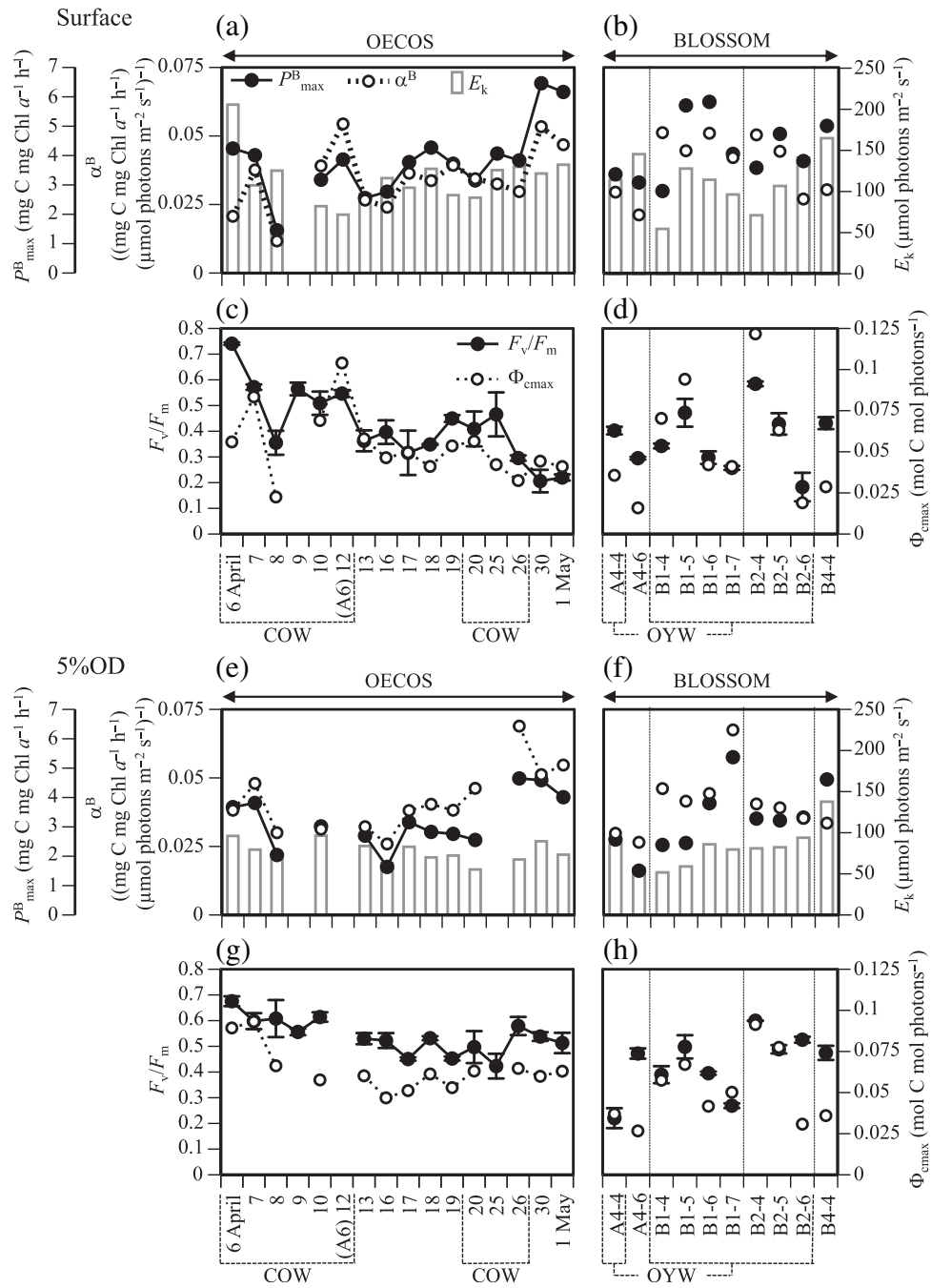


Fig. 9. Changes in (a, b and e, f) maximum photosynthetic rate (P_{max}^B), initial slope (α^B) of the PE curve, the light saturation index (E_k), (c, d and g, h) maximum photochemical efficiency (F_v/F_m) of the algal PSII and maximum quantum yield of carbon fixation in photosynthesis (Φ_{cmax}) at (a–d) the surface and (e–h) 5% optical depth (OD) in this study. COW and OYW with dashed lines are as in Fig. 4.

results were consistent with Argo float data collected during the same period (Okamoto et al. 2010). The Argo data showed that there was no bloom ($< 1.5 \text{ mg m}^{-3}$) in the eastern part of Oyashio region during April 2007, but Chl *a* concentration almost increased twofold from winter, explained by the critical depth hypothesis (Sverdrup 1953). However, from the middle of May to June 2007, we found that diatoms flourished

under low DFe concentrations (Table 1) at Stns. B1 and B2 of OYW in the eastern part of Oyashio region. Interestingly, although cluster analysis (Fig. 7a) based on diatom taxa mainly classified Stns. B1-5 and B2-5 of OYW in the middle of May into the OECOS group because of the predominance of *Thalassiosira* species, our RDA results (Fig. 7b) indicated that the different environmental factors were associated with the

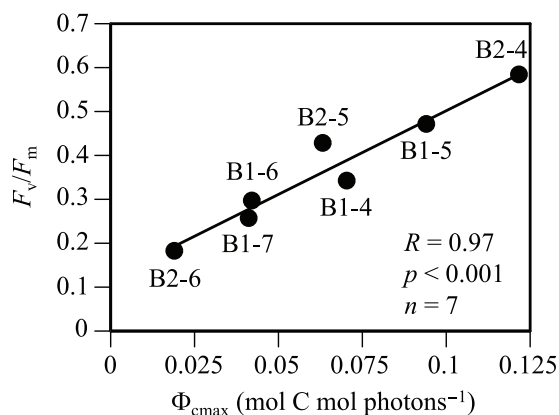


Fig. 10. Relationships between F_v/F_m and Φ_{cmax} at the surface at Stns. B1 and B2 in the OYW during the BLOSSOM cruises.

OECOS and BLOSSOM diatom species composition. Higher DFe concentrations and lower temperatures, corresponding with the high contribution of COW to the observed water masses, affected the diatom community during OECOS, especially on 06 April–08 April and 12 April. In contrast, the diatom assemblages observed during BLOSSOM including Stns. B1-5 and B2-5 of OYW were not correlated with DFe concentrations. These results indicated that diatoms in the OYW possess different adaptation strategies for low iron conditions as compared with diatoms in the water masses affected by COW. Our findings suggested that iron mainly controls the remarkable east–west contrast of Chl *a* concentration within the Oyashio region and that both iron and other environmental factors affected the initiation of the spring bloom in the eastern part of the Oyashio region. However, the main factors regulating the initiation of the bloom in the eastern part of the Oyashio region are still unclear because hydrographic conditions of OYW at Stns. B1 and B2 in May 2007 were quite similar before and after the intensive bloom (Table 1).

Conclusions

Our study highlights the importance of high resolution water mass characterization in conjunction with detailed taxonomic and physiological assessments of phytoplankton for further understanding of marine ecosystems. High frequency observations during spring in the Oyashio region showed that a massive diatom bloom occurred in the water mass influenced by the COW in April, whereas an intensive bloom was not found until the middle of May in the OYW in the eastern part of the Oyashio region. This was probably due to lower DFe concentration in the OYW than in the COW. Other environmental factors such as light availability (Saito and Tsuda 2003) and vertical dilution by winter mixing (Yoshie et al. 2003) could also delay the intensive bloom initiation in the eastern part of the Oyashio region where the influence of coastal Oyashio water is small. This in turn led to the spatial

heterogeneity of the spring bloom in the Oyashio region. Additionally, the spatial heterogeneity of the Oyashio spring bloom could be related to different adaptive strategies to mitigate iron deficiency between diatom assemblages of the COW and OYW. It is known that trace metals requirements are distinct between coastal and oceanic diatoms (Strzepek and Harrison 2004; Peers and Price 2006). However, our immunological Fd/Fld assay could not be used as a diagnostic of Fe deficiency in micro-sized diatoms during the spring bloom in the Oyashio region. Recently, Chappell et al. (2015) proposed alternative methods for evaluating iron limitation using the genes encoding flavodoxin (*FLDA1*) and Fe-starvation induced protein 3 (*ISIP3*). Marchetti et al. (2017) also proposed a new index, the *Pseudo-nitzschia* Iron Limitation Index (*Ps-n* ILL), based on a comparative transcriptomic approach using gene sequences of ferritin (*FTN*), encoding the iron storage protein, and iron-starvation-induced protein 2a (*ISIP2a*), encoding an iron-concentrating protein. They suggested that chronically iron-limited diatom communities do not use ferredoxin or may have lost the gene for ferredoxin to adapt to low Fe conditions. These approaches may lead to better understanding for adaptation strategies of diatoms to variable Fe conditions in the COW and OYW. Our results also emphasize the necessity for further studying the seasonal and annual changes in physicochemical properties and the composition and photosynthetic features of phytoplankton in the COW and OYW to better understand blooming dynamics of the Oyashio ecosystem.

References

- Behrenfeld, M. J., K. Worthington, R. M. Sherrell, F. P. Chavez, P. Strutton, M. McPhaden, and D. M. Shea. 2006. Controls on tropical Pacific Ocean productivity revealed through nutrient stress diagnostics. *Nature* **442**: 1025–1028. doi:10.1038/nature05083
- Behrenfeld, M. J., K. H. Halsey, and A. J. Milligan. 2008. Evolved physiological responses of phytoplankton to their integrated growth environment. *Philos. Trans. R. Soc. B* **363**: 2687–2703. doi:10.1098/rstb.2008.0019
- Behrenfeld, M. J., and A. J. Milligan. 2013. Photophysiological expressions of iron stress in phytoplankton. *Ann. Rev. Mar. Sci.* **5**: 217–246. doi:10.1146/annurev-marine-121211-172356
- Boyd, P., J. LaRoche, M. Gall, R. Frew, and R. M. L. McKay. 1999. Role of iron, light, and silicate in controlling algal biomass in subantarctic waters SE of New Zealand. *J. Geophys. Res.* **104**: 13395–13408. doi:10.1029/1999JC900009
- Boyd, P. W. and others 2004. The decline and fate of an iron-induced subarctic phytoplankton bloom. *Nature* **428**: 549–553. doi:10.1038/nature02437
- Boyd, P. W. and others 2005. The evolution and termination of an iron-induced mesoscale bloom in the northeast

- subarctic Pacific. *Limnol. Oceanogr.* **50**: 1872–1886. doi:[10.4319/lo.2005.50.6.1872](https://doi.org/10.4319/lo.2005.50.6.1872)
- Boyd, P. W. and others 2007. Mesoscale iron enrichment experiments 1993–2005: Synthesis and future directions. *Science* **315**: 612–617. doi:[10.1126/science.1131669](https://doi.org/10.1126/science.1131669)
- Carradec, Q. and others 2018. A global ocean atlas of eukaryotic genes. *Nat. Commun.* **9**: 373. doi:[10.1038/s41467-017-02342-1](https://doi.org/10.1038/s41467-017-02342-1)
- Chappell, P. D., L. P. Whitney, J. R. Wallace, A. I. Darer, S. Jean-Charles, and B. D. Jenkins. 2015. Genetic indicators of iron limitation in wild populations of *Thalassiosira oceanica* from the northeast Pacific Ocean. *ISME J.* **9**: 592–602. doi:[10.1038/ismej.2014.171](https://doi.org/10.1038/ismej.2014.171)
- Chiba, S., T. Ono, K. Tadokoro, T. Midorikawa, and T. Saino. 2004. Increased stratification and decreased lower trophic level productivity in the Oyashio region of the North Pacific: A 30-year retrospective study. *J. Oceanogr.* **60**: 149–162. doi:[10.1023/B:JOCE.0000038324.14054.cf](https://doi.org/10.1023/B:JOCE.0000038324.14054.cf)
- Chierici, M., A. Fransson, and Y. Nojiri. 2006. Biogeochemical processes as drivers of surface fCO_2 in contrasting provinces in the subarctic North Pacific Ocean. *Global Biogeochem. Cycles* **20**: GB1009. doi:[10.1029/2004GB002356](https://doi.org/10.1029/2004GB002356)
- Davey, M., and R. J. Geider. 2001. Impact of iron limitation on the photosynthetic apparatus of the diatom *Chaetoceros muelleri* (Bacillariophyceae). *J. Phycol.* **37**: 987–1000. doi:[10.1046/j.1529-8817.2001.99169.x](https://doi.org/10.1046/j.1529-8817.2001.99169.x)
- Falkowski, P. G., D. Ziemann, Z. Kolber, and P. K. Bienfang. 1991. Role of eddy pumping in enhancing primary production in the ocean. *Nature* **352**: 55–58. doi:[10.1038/352055a0](https://doi.org/10.1038/352055a0)
- Food and Agriculture Organization (FAO) of the United Nations. 2016. The State of World Fisheries and Aquaculture. Contributing to food security and nutrition for all, p. 200. FAO.
- Grossman, R. D., M. S. Parker, and E. V. Armbrust. 2015. Diversity and evolutionary history of iron metabolism genes in diatoms. *PLoS One* **10**: e0129081. doi:[10.1371/journal.pone.0129081](https://doi.org/10.1371/journal.pone.0129081)
- Gruber, N., Z. Lachkar, H. Frenzel, P. Marchesiello, M. Münnich, J. C. McWilliams, T. Nagai, and G.-K. Plattner. 2011. Eddy-induced reduction of biological production in eastern boundary upwelling systems. *Nat. Geosci.* **4**: 787–792. doi:[10.1038/ngeo1273](https://doi.org/10.1038/ngeo1273)
- Halsey, K. H., A. J. Milligan, and M. J. Behrenfeld. 2010. Physiological optimization underlies growth rate-independent chlorophyll-specific gross and net primary production. *Photosynth. Res.* **103**: 125–137. doi:[10.1007/s11120-009-9526-z](https://doi.org/10.1007/s11120-009-9526-z)
- Halsey, K. H., R. T. O'Malley, J. R. Graff, A. J. Milligan, and M. J. Behrenfeld. 2013. A common partitioning strategy for photosynthetic products in evolutionarily distinct phytoplankton species. *New Phytol.* **198**: 1030–1038. doi:[10.1111/nph.12209](https://doi.org/10.1111/nph.12209)
- Halsey, K. H., and B. M. Jones. 2015. Phytoplankton strategies for photosynthetic energy allocation. *Ann. Rev. Mar. Sci.* **7**: 265–297. doi:[10.1146/annurev-marine-010814-015813](https://doi.org/10.1146/annurev-marine-010814-015813)
- Hama, T., T. Miyazaki, Y. Ogawa, T. Iwakuma, M. Takahashi, A. Otsuki, and S. Ichimura. 1983. Measurement of photosynthetic production of a marine phytoplankton population using a stable ^{13}C isotope. *Mar. Biol.* **73**: 31–36. doi:[10.1007/BF00396282](https://doi.org/10.1007/BF00396282)
- Hanawa, K., and H. Mitsudera. 1987. Variation of water system distribution in the Sanriku coastal area. *J. Oceanogr.* **42**: 435–446. doi:[10.1007/BF02110194](https://doi.org/10.1007/BF02110194)
- Harrison, P. J., P. W. Boyd, D. E. Varela, S. Takeda, A. Shiimoto, and T. Odate. 1999. Comparison of factors controlling phytoplankton productivity in the NE and NW subarctic Pacific gyres. *Prog. Oceanogr.* **43**: 205–234. doi:[10.1016/S0079-6611\(99\)00015-4](https://doi.org/10.1016/S0079-6611(99)00015-4)
- Harrison, P. J., F. A. Whitney, A. Tsuda, H. Saito, and K. Tadokoro. 2004. Nutrient and plankton dynamics in the NE and NW gyres of the subarctic Pacific Ocean. *J. Oceanogr.* **60**: 93–117. doi:[10.1023/B:JOCE.0000038321.57391.2a](https://doi.org/10.1023/B:JOCE.0000038321.57391.2a)
- Hattori, H., M. Koike, K. Tachikawa, H. Saito, and K. Nagasawa. 2004. Spatial variability of living coccolithophore distribution in the western subarctic Pacific and western Bering Sea. *J. Oceanogr.* **60**: 505–515. doi:[10.1023/B:JOCE.0000038063.81738.ab](https://doi.org/10.1023/B:JOCE.0000038063.81738.ab)
- Hattori-Saito, A., J. Nishioka, T. Ono, R. M. L. McKay, and K. Suzuki. 2010. Iron deficiency in micro-sized diatoms in the Oyashio region of the western subarctic Pacific during spring. *J. Oceanogr.* **66**: 105–115. doi:[10.1007/s10872-010-0009-9](https://doi.org/10.1007/s10872-010-0009-9)
- Hutchins, D. A., and K. W. Bruland. 1998. Iron-limited diatom growth and Si:N uptake ratios in a coastal upwelling regime. *Nature* **393**: 561–564. doi:[10.1038/31203](https://doi.org/10.1038/31203)
- Ikeda, T., N. Shiga, and A. Yamaguchi. 2008. Structure, biomass, distribution and trophodynamics of the pelagic ecosystem in the Oyashio region, western subarctic Pacific. *J. Oceanogr.* **64**: 339–354. doi:[10.1007/s10872-008-0027-z](https://doi.org/10.1007/s10872-008-0027-z)
- Ikeda, T., A. Yamaguchi, and C. B. Miller. 2010. Oceanic Ecosystems Comparison Subarctic-Pacific (OECOS): West. *Deep-Sea Res. Part II* **57**: 1593–1594. doi:[10.1016/j.dsr2.2010.03.003](https://doi.org/10.1016/j.dsr2.2010.03.003)
- Isada, T., A. Kuwata, H. Saito, T. Ono, M. Ishii, H. Yoshikawa-Inoue, and K. Suzuki. 2009. Photosynthetic features and primary productivity of phytoplankton in the Oyashio and Kuroshio–Oyashio transition regions of the northwest Pacific. *J. Plankton Res.* **31**: 1009–1025. doi:[10.1093/plankt/fbp050](https://doi.org/10.1093/plankt/fbp050)
- Isada, T., A. Hattori-Saito, H. Saito, T. Ikeda, and K. Suzuki. 2010. Primary productivity and its bio-optical modeling in the Oyashio region, NW Pacific during the spring bloom 2007. *Deep-Sea Res. Part II* **57**: 1653–1664. doi:[10.1016/j.dsr2.2010.03.009](https://doi.org/10.1016/j.dsr2.2010.03.009)
- Isada, T., T. Iida, H. Liu, S.-I. Saitoh, J. Nishioka, T. Nakatsuka, and K. Suzuki. 2013. Influence of Amur River discharge on phytoplankton photophysiology in the Sea of Okhotsk during late summer. *J. Geophys. Res. Oceans* **118**: 1995–2013. doi:[10.1002/jgrc.20159](https://doi.org/10.1002/jgrc.20159)

- Itoh, S., and I. Yasuda. 2010. Characteristics of mesoscale eddies in the Kuroshio–Oyashio extension region detected from the distribution of the sea surface height anomaly. *J. Phys. Oceanogr.* **40**: 1018–1034. doi:[10.1175/2009JPO4265.1](https://doi.org/10.1175/2009JPO4265.1)
- Kasai, H., H. Saito, A. Yoshimori, and S. Taguchi. 1997. Variability in timing and magnitude of spring bloom in the Oyashio region, the western subarctic Pacific off Hokkaido, Japan. *Fish. Oceanogr.* **6**: 118–129. doi:[10.1046/j.1365-2419.1997.00034.x](https://doi.org/10.1046/j.1365-2419.1997.00034.x)
- Kono, T., and M. Sato. 2010. A mixing analysis of surface water in the Oyashio region: Its implications and application to variations of the spring bloom. *Deep-Sea Res. Part II* **57**: 1595–1607. doi:[10.1016/j.dsr2.2010.03.004](https://doi.org/10.1016/j.dsr2.2010.03.004)
- Kusaka, A., T. Azumaya, and Y. Kawasaki. 2013. Monthly variations of hydrographic structures and water mass distribution off the Doto area, Japan. *J. Oceanogr.* **69**: 295–312. doi:[10.1007/s10872-013-0174-8](https://doi.org/10.1007/s10872-013-0174-8)
- La Roche, J., P. W. Boyd, R. M. L. McKay, and R. J. Geider. 1996. Flavodoxin as an in situ marker for iron stress in phytoplankton. *Nature* **382**: 802–805. doi:[10.1038/382802a0](https://doi.org/10.1038/382802a0)
- Lawrenz, E. and others 2013. Predicting the electron requirement for carbon fixation in seas and oceans. *PLoS One* **8**: e58137. doi:[10.1371/journal.pone.0058137](https://doi.org/10.1371/journal.pone.0058137)
- Levitus, S. 1982. Climatological atlas of the world ocean, 173 p. NOAA Professional Paper 13.
- Mahadevan, A. 2016. The impact of submesoscale physics on primary production of plankton. *Ann. Rev. Mar. Sci.* **8**: 161–184. doi:[10.1146/annurev-marine-010814-015912](https://doi.org/10.1146/annurev-marine-010814-015912)
- Marchetti, A. and others 2012. Comparative metatranscriptomics identifies molecular bases for the physiological responses of phytoplankton to varying iron availability. *Proc. Natl. Acad. Sci. USA* **109**: E317–E325. doi:[10.1073/pnas.1118408109](https://doi.org/10.1073/pnas.1118408109)
- Marchetti, A., and M. T. Maldonado. 2016. Iron, p. 233–279. *In* M. A. Borowitzka, J. Beardall, and J. A. Raven [eds.], *The physiology of microalgae*. Springer.
- Marchetti, A., C. M. Moreno, N. R. Cohen, I. Oleinikou, K. deLong, B. S. Twining, E. V. Armbrust, and R. H. Lampe. 2017. Development of a molecular-based index for assessing iron status in bloom-forming pennate diatoms. *J. Phycol.* **53**: 820–832. doi:[10.1111/jpy.12539](https://doi.org/10.1111/jpy.12539)
- McKay, R. M. L., R. J. Geider, and J. La Roche. 1997. Physiological and biochemical response of the photosynthetic apparatus of two marine diatoms to Fe stress. *Plant Physiol.* **114**: 615–622. doi:[10.1104/pp.114.2.615](https://doi.org/10.1104/pp.114.2.615)
- Milligan, A. J., K. H. Halsey, and M. J. Behrenfeld. 2015. Advancing interpretations of ¹⁴C-uptake measurements in the context of phytoplankton physiology and ecology. *J. Plankton Res.* **37**: 692–698. doi:[10.1093/plankt/fbv051](https://doi.org/10.1093/plankt/fbv051)
- Moore, C. M., M. M. Mills, A. Milne, R. Langlois, E. P. Achterberg, K. Lochte, R. J. Geider, and J. La Roche. 2006. Iron limits primary productivity during spring bloom development in the central North Atlantic. *Glob. Chang. Biol.* **12**: 626–634. doi:[10.1111/j.1365-2486.2006.01122.x](https://doi.org/10.1111/j.1365-2486.2006.01122.x)
- Nakayama, Y., K. Kuma, S. Fujita, K. Sugie, and T. Ikeda. 2010. Temporal variability and bioavailability of iron and other nutrients during the spring phytoplankton bloom in the Oyashio region. *Deep-Sea Res. Part II* **57**: 1618–1629. doi:[10.1016/j.dsr2.2010.03.006](https://doi.org/10.1016/j.dsr2.2010.03.006)
- Nishioka, J. and others 2007. Iron supply to the western subarctic Pacific: Importance of iron export from the Sea of Okhotsk. *J. Geophys. Res.* **112**: C10012. doi:[10.1029/2006JC004055](https://doi.org/10.1029/2006JC004055)
- Nishioka, J., T. Ono, H. Saito, K. Sakaoka, and T. Yoshimura. 2011. Oceanic iron supply mechanisms which support the spring diatom bloom in the Oyashio region, western subarctic Pacific. *J. Geophys. Res.* **116**: C02021. doi:[10.1029/2010JC006321](https://doi.org/10.1029/2010JC006321)
- Nishioka, J., and H. Obata. 2017. Dissolved iron distribution in the western and central subarctic Pacific: HNLC water formation and biogeochemical processes. *Limnol. Oceanogr.* **62**: 2004–2022. doi:[10.1002/lno.10548](https://doi.org/10.1002/lno.10548)
- Nosaka, Y., Y. Yamashita, and K. Suzuki. 2017. Dynamics and origin of transparent exopolymer particles in the Oyashio region of the western subarctic Pacific during the spring diatom bloom. *Front. Mar. Sci.* **4**: 79. doi:[10.3389/fmars.2017.00079](https://doi.org/10.3389/fmars.2017.00079)
- Obata, H., H. Karatani, and E. Nakayama. 1993. Automated determination of iron in seawater by chelating resin concentration and chemiluminescence detection. *Anal. Chem.* **65**: 1524–1528. doi:[10.1021/ac00059a007](https://doi.org/10.1021/ac00059a007)
- Ohtani, K., Y. Akiba, K. Yoshida, and T. Ohtsuki. 1971. Studies on the change of the hydrographic conditions in the Funka bay III. Oceanographic conditions of the Funka bay occupied by the Oyashio waters. *Bull. Fac. Fish. Hokkaido Univ.* **22**: 58–66 (in Japanese with English abstract).
- Okamoto, S., T. Hirawake, and S.-I. Saitoh. 2010. Interannual variability in the magnitude and timing of the spring bloom in the Oyashio region. *Deep-Sea Res. Part II* **57**: 1608–1617. doi:[10.1016/j.dsr2.2010.03.005](https://doi.org/10.1016/j.dsr2.2010.03.005)
- Oksanen, J., and others. 2018. *Vegan: Community Ecology Package*. R Package Version 2.5-1. Available from <https://CRAN.R-project.org/package=vegan>
- Peers, G., and N. M. Price. 2006. Copper-containing plastocyanin used for electron transport by an oceanic diatom. *Nature* **441**: 341–344. doi:[10.1038/nature04630](https://doi.org/10.1038/nature04630)
- Platt, T., C. L. Gallegos, and W. G. Harrison. 1980. Photoinhibition of photosynthesis in natural assemblages of marine phytoplankton. *J. Mar. Res.* **38**: 687–701.
- R Core Team 2018. *R: A language and environment for statistical computing*. R Foundation for Statistical Computing, Vienna, Austria. URL <https://www.R-project.org/>.
- Revelle, W. 2018. *Psych: Procedures for psychological, psychometric, and personality research*. R Package Version 1.8.3.3. Available from <https://CRAN.R-project.org/package=psych>
- Saito, H., A. Tsuda, and H. Kasai. 2002. Nutrient and plankton dynamics in the Oyashio region of the western subarctic

- Pacific Ocean. *Deep-Sea Res. Part II* **49**: 5463–5486. doi:[10.1016/S0967-0645\(02\)00204-7](https://doi.org/10.1016/S0967-0645(02)00204-7)
- Saito, H., and A. Tsuda. 2003. Influence of light intensity on diatom physiology and nutrient dynamics in the Oyashio region. *Prog. Oceanogr.* **57**: 251–263. doi:[10.1016/S0079-6611\(03\)00100-9](https://doi.org/10.1016/S0079-6611(03)00100-9)
- Sakamoto, K., H. Tsujino, S. Nishikawa, H. Nakano, and T. Motoi. 2010. Dynamics of the Coastal Oyashio and its seasonal variation in a high-resolution western North Pacific Ocean model. *J. Phys. Oceanogr.* **40**: 1283–1301. doi:[10.1175/2010JPO4307.1](https://doi.org/10.1175/2010JPO4307.1)
- Sakurai, Y. 2007. An overview of the Oyashio ecosystem. *Deep-Sea Res. Part II* **54**: 2526–2542. doi:[10.1016/j.dsr2.2007.02.007](https://doi.org/10.1016/j.dsr2.2007.02.007)
- Sato, M., and K. Furuya. 2010. Pico- and nanophytoplankton dynamics during the decline phase of the spring bloom in the Oyashio region. *Deep-Sea Res. Part II* **57**: 1643–1652. doi:[10.1016/j.dsr2.2010.03.008](https://doi.org/10.1016/j.dsr2.2010.03.008)
- Shinada, A., N. Shiga, and S. Ban. 1999a. Structure and magnitude of diatom spring bloom in Funka Bay, southwestern Hokkaido, Japan, as influenced by the intrusion of Coastal Oyashio Water. *Plankton Biol. Ecol.* **46**: 24–29.
- Shinada, A., N. Shiga, and S. Ban. 1999b. Origin of *Thalassiosira* diatoms that cause the spring phytoplankton bloom in Funka Bay, southwestern Hokkaido, Japan. *Plankton Biol. Ecol.* **46**: 89–93.
- Shiomoto, A. 2000. Efficiency of water-column light utilization in the subarctic northwestern Pacific. *Limnol. Oceanogr.* **45**: 982–987. doi:[10.4319/lo.2000.45.4.0982](https://doi.org/10.4319/lo.2000.45.4.0982)
- Shiozaki, T., S. Ito, K. Takahashi, H. Saito, T. Nagata, and K. Furuya. 2014. Regional variability of factors controlling the onset timing and magnitude of spring algal blooms in the northwestern North Pacific. *J. Geophys. Res.* **119**: 253–265. doi:[10.1002/2013JC009187](https://doi.org/10.1002/2013JC009187)
- Silsbe, G. M., and J. C. Kromkamp. 2012. Modeling the irradiance dependency of the quantum efficiency of photosynthesis. *Limnol. Oceanogr.: Methods* **10**: 645–652. doi:[10.4319/lom.2012.10.645](https://doi.org/10.4319/lom.2012.10.645)
- Silsbe, G. M., and S. Y. Malkin. 2015. Phytotools: Phytoplankton production tools. R package Version 1.0. Available from <https://CRAN.R-project.org/package=phytotools>
- Strzepek, R. F., and P. J. Harrison. 2004. Photosynthetic architecture differs in coastal and oceanic diatoms. *Nature* **431**: 689–692. doi:[10.1038/nature02954](https://doi.org/10.1038/nature02954)
- Suga, T., K. Motoki, and Y. Aoki. 2004. The North Pacific climatology of winter mixed layer and mode waters. *J. Phys. Oceanogr.* **34**: 3–22. doi:[10.1175/1520-0485\(2004\)034<0003:TNPCOW>2.0.CO;2](https://doi.org/10.1175/1520-0485(2004)034<0003:TNPCOW>2.0.CO;2)
- Sugie, K., K. Kuma, S. Fujita, Y. Nakayama, and T. Ikeda. 2010. Nutrient and diatom dynamics during late winter and spring in the Oyashio region of the western subarctic Pacific Ocean. *Deep-Sea Res. Part II* **57**: 1630–1642. doi:[10.1016/j.dsr2.2010.03.007](https://doi.org/10.1016/j.dsr2.2010.03.007)
- Suzuki, K., H. Liu, T. Saino, H. Obata, M. Takano, K. Okamura, Y. Sohrin, and Y. Fujishima. 2002. East–west gradients in the photosynthetic potential of phytoplankton and iron concentration in the subarctic Pacific Ocean during early summer. *Limnol. Oceanogr.* **47**: 1581–1594. doi:[10.4319/lo.2002.47.6.1581](https://doi.org/10.4319/lo.2002.47.6.1581)
- Suzuki, K., A. Hinuma, H. Saito, H. Kiyosawa, H. Liu, T. Saino, and A. Tsuda. 2005. Responses of phytoplankton and heterotrophic bacteria in the northwest subarctic Pacific to in situ iron fertilization as estimated by HPLC pigment analysis and flow cytometry. *Prog. Oceanogr.* **64**: 167–187. doi:[10.1016/j.pocean.2005.02.007](https://doi.org/10.1016/j.pocean.2005.02.007)
- Suzuki, K. and others 2009. Community structure and photosynthetic physiology of phytoplankton in the northwest subarctic Pacific during an in situ iron fertilization experiment (SEEDS-II). *Deep-Sea Res. Part II* **56**: 2733–2744. doi:[10.1016/j.dsr2.2009.06.001](https://doi.org/10.1016/j.dsr2.2009.06.001)
- Suzuki, K., A. Kuwata, N. Yoshie, A. Shibata, K. Kawanobe, and H. Saito. 2011. Population dynamics of phytoplankton, heterotrophic bacteria, and viruses during the spring bloom in the western subarctic Pacific. *Deep-Sea Res. Part I* **58**: 575–589. doi:[10.1016/j.dsr.2011.03.003](https://doi.org/10.1016/j.dsr.2011.03.003)
- Suzuki, K., A. Hattori-Saito, Y. Sekiguchi, J. Nishioka, M. Shigemitsu, T. Isada, H. Liu, and R. M. L. McKay. 2014. Spatial variability in iron nutritional status of large diatoms in the Sea of Okhotsk with special reference to the Amur River discharge. *Biogeosciences* **11**: 2503–2517. doi:[10.5194/bg-11-2503-2014](https://doi.org/10.5194/bg-11-2503-2014)
- Suzuki, R., and T. Ishimaru. 1990. An improved method for the determination of phytoplankton chlorophyll using N, N-dimethylformamide. *J. Oceanogr.* **46**: 190–194. doi:[10.1007/BF02125580](https://doi.org/10.1007/BF02125580)
- Sverdrup, H. 1953. On conditions for the vernal blooming of phytoplankton. *J. Conseil Int. Explor. Mer* **18**: 287–295.
- Takahashi, T. and others 2002. Global sea-air CO₂ flux based in climatological surface ocean pCO₂, and seasonal biological and temperature effects. *Deep-Sea Res. Part II* **49**: 1601–1622. doi:[10.1016/S0967-0645\(02\)00003-6](https://doi.org/10.1016/S0967-0645(02)00003-6)
- Taniguchi, A. 1999. Differences in the structure of the lower trophic levels of pelagic ecosystems in the eastern and western subarctic Pacific. *Prog. Oceanogr.* **43**: 289–315. doi:[10.1016/S0079-6611\(99\)00011-7](https://doi.org/10.1016/S0079-6611(99)00011-7)
- Tomas, C. R. 1997. Identifying marine phytoplankton. Academic Press.
- Tsuda, A. and others 2003. A mesoscale iron enrichment in the western subarctic Pacific induces large centric diatom bloom. *Science* **300**: 958–961. doi:[10.1126/science.1082000](https://doi.org/10.1126/science.1082000)
- Tsuda, A. and others 2005. Responses of diatoms to iron-enrichment (SEEDS) in the western subarctic Pacific, temporal and spatial comparisons. *Prog. Oceanogr.* **64**: 189–205. doi:[10.1016/j.pocean.2005.02.008](https://doi.org/10.1016/j.pocean.2005.02.008)
- Tsuda, A. and others 2007. Evidence for the grazing hypothesis: Grazing reduces phytoplankton responses of the HNLC ecosystem to iron enrichment in the western subarctic

- Pacific (SEEDS II). *J. Oceanogr.* **63**: 983–994. doi:[10.1007/s10872-007-0082-x](https://doi.org/10.1007/s10872-007-0082-x)
- Welschmeyer, N. A. 1994. Fluorometric analysis of chlorophyll-a in the presence of chlorophyll-b and phaeopigments. *Limnol. Oceanogr.* **39**: 1985–1992. doi:[10.4319/lo.1994.39.8.1985](https://doi.org/10.4319/lo.1994.39.8.1985)
- Whitney, L. P., J. J. Lins, M. P. Hughes, M. L. Wells, P. D. Chappell, and B. D. Jenkins. 2011. Characterization of putative iron responsive genes as species-specific indicators of iron stress in *Thalassiosiroid* diatoms. *Front. Microbiol.* **2**: 1–14. doi:[10.3389/fmicb.2011.00234](https://doi.org/10.3389/fmicb.2011.00234)
- Wright, S. W., S. W. Jeffrey, R. F. C. Mantoura, C. A. Llewellyn, T. Bjørnland, D. Repeta, and N. Welschmeyer. 1991. Improved HPLC method for the analysis of chlorophylls and carotenoids from marine phytoplankton. *Mar. Ecol. Prog. Ser.* **77**: 183–196. doi:[10.3354/meps077183](https://doi.org/10.3354/meps077183)
- Wright, S. W., A. Ishikawa, H. J. Marchant, A. T. Davidson, R. L. van den Enden, and G. V. Nash. 2009. Composition and significance of picophytoplankton in Antarctic waters. *Polar Biol.* **32**: 797–808. doi:[10.1007/s00300-009-0582-9](https://doi.org/10.1007/s00300-009-0582-9)
- Yasuda, I. 2003. Hydrographic structure and variability in the Kuroshio-Oyashio transition area. *J. Oceanogr.* **59**: 389–402. doi:[10.1023/A:1025580313836](https://doi.org/10.1023/A:1025580313836)
- Yasuda, I. 2004. North Pacific intermediate water: Progress in SAGE (SubArctic Gyre Experiment) and related projects. *J. Oceanogr.* **60**: 385–395. doi:[10.1023/B:JOCE.0000038344.25081.42](https://doi.org/10.1023/B:JOCE.0000038344.25081.42)
- Yoshie, N., Y. Yamanaka, M. J. Kishi, and H. Saito. 2003. One dimensional ecosystem model simulation of the effects of vertical dilution by the winter mixing on the spring diatom bloom. *J. Oceanogr.* **59**: 563–571. doi:[10.1023/B:JOCE.0000009586.02554.d3](https://doi.org/10.1023/B:JOCE.0000009586.02554.d3)
- Yoshie, N., K. Suzuki, A. Kuwata, J. Nishioka, and H. Saito. 2010. Temporal and spatial variations in photosynthetic physiology of diatoms during the spring bloom in the western subarctic Pacific. *Mar. Ecol. Prog. Ser.* **399**: 39–52. doi:[10.3354/meps08329](https://doi.org/10.3354/meps08329)

Acknowledgment

We thank the officers and crews of R/V *Hakuho Maru* and FR/V *Wakataka Maru* for their helpful assistance. We gratefully acknowledge Prof. S.-I. Saitoh for kind loan of the spectroradiometer. Dr. H. Kasai helped with EA-MS analysis. We would like to extend our thanks the members of the OECOS and BLOSSOM projects for their assistance during our sampling and useful comments. We are also grateful to two anonymous reviewers for their valuable comments and suggestions on the manuscript. This work was supported by a Sasakawa Scientific Research Grant from the Japan Science Society to T.I. and A.H. and by the Steel Industry Foundation for the Advancement of Environmental Protection Technology to K.S.

Conflict of Interest

None declared.

Submitted 29 November 2017

Revised 16 May 2018

Accepted 20 July 2018

Associate editor: James Moffett